

# Inclusive Charm Production in $\chi_b$ Decays

Geoffrey T. Bodwin,<sup>1</sup> Eric Braaten,<sup>2</sup> Daekyoung Kang,<sup>2,3</sup> and Jungil Lee<sup>1,3</sup>

<sup>1</sup> *High Energy Physics Division, Argonne National Laboratory,  
9700 S. Cass Avenue, Argonne, Illinois 60439, USA*

<sup>2</sup> *Physics Department, Ohio State University, Columbus, Ohio 43210, USA*

<sup>3</sup> *Department of Physics, Korea University, Seoul 136-701, Korea*

(Dated: February 1, 2008)

## Abstract

We calculate the inclusive decay rate of the spin-triplet bottomonium states  $\chi_{bJ}$  into charm hadrons, including the leading-order color-singlet and color-octet  $b\bar{b}$  annihilation mechanisms. We also calculate the momentum distribution of the charm quark from the decay of  $\chi_{bJ}$ . The infrared divergences from the color-singlet process  $b\bar{b} \rightarrow c\bar{c}g$  are factored into the probability density at the origin for a  $b\bar{b}$  pair in a color-octet state. That probability density can be determined phenomenologically from the fraction of decays of  $\chi_{bJ}$  that include charm hadrons. It can then be used to predict the partial widths into light hadrons for all four states in the  $P$ -wave bottomonium multiplet.

PACS numbers: 12.38.-t, 12.39.St, 13.20.Gd, 14.40.Gx

## I. INTRODUCTION

The asymptotic freedom of QCD suggests that the total widths of heavy quarkonium states should be calculable using perturbation theory. The earliest calculations of the widths of  $P$ -wave quarkonium states using perturbative QCD were plagued with infrared divergences [1–3]. The calculations were based on a factorization assumption that the width could be expressed as the product of  $|R'(0)|^2$ , where  $R'(0)$  is the derivative of the radial wave function at the origin, and a perturbatively calculable coefficient. However the coefficients were found to be infrared divergent at leading order in  $\alpha_s$  for the spin-1 states and at next-to-leading order in  $\alpha_s$  for the spin-0 and spin-2 states. The infrared divergences were often expressed in terms of a logarithmic dependence on the binding energy of the quarkonium, a quantity that is not calculable using perturbation theory. However the correct interpretation of the infrared divergences is that they reveal the failure of the factorization assumption.

This problem was overcome in 1992 when Bodwin, Braaten, and Lepage showed that the infrared divergences could be absorbed into the probability for the heavy-quark-antiquark ( $Q\bar{Q}$ ) pair to be at the same point in a color-octet state [4]. They used a nonrelativistic effective field theory for the  $Q\bar{Q}$  sector of QCD called NRQCD to derive a general factorization formula for inclusive quarkonium decay rates [5]. A  $P$ -wave multiplet consists of four heavy quarkonium states:  $\chi_{Q0}$ ,  $\chi_{Q1}$ ,  $\chi_{Q2}$ , and  $h_Q$  with  $J^{PC}$  quantum numbers  $0^{++}$ ,  $1^{++}$ ,  $2^{++}$ , and  $1^{+-}$ , respectively. At leading order in the velocity  $v$  of the heavy quark or antiquark in the quarkonium rest frame, there are only two independent nonperturbative factors in the annihilation decay rates of all four states in the  $P$ -wave multiplet:  $\langle\mathcal{O}_1\rangle$ , which is proportional to  $|R'(0)|^2$ , and  $\langle\mathcal{O}_8\rangle$ , which is proportional to the probability for the  $Q$  and  $\bar{Q}$  to be at the same point in a color-octet state. These nonperturbative factors can be expressed as matrix elements of local four-quark operators in NRQCD. The short-distance coefficients of the NRQCD matrix elements can be calculated as power series in the QCD coupling constant  $\alpha_s$ .

The widths of all four states in a  $P$ -wave multiplet can be calculated by using the NRQCD factorization formula, once the two nonperturbative factors  $\langle\mathcal{O}_1\rangle$  and  $\langle\mathcal{O}_8\rangle$  have been determined. These matrix elements can be calculated by using lattice simulations of NRQCD. An alternative is to estimate the color-singlet matrix element  $\langle\mathcal{O}_1\rangle$  by using potential models and to determine the color-octet matrix element  $\langle\mathcal{O}_8\rangle$  phenomenologically. The phenom-

logical determination of  $\langle \mathcal{O}_8 \rangle$  requires the measurement of an observable that is sensitive to this matrix element. In the case of bottomonium, one such observable is the inclusive rate for charm production in decays of the spin-triplet  $P$ -wave states  $\chi_{bJ}$ . This rate is sensitive to  $\langle \mathcal{O}_8 \rangle$  because the production of charm quarks from  $b\bar{b}$  annihilation in the color-singlet channel is suppressed by a factor of  $\alpha_s$ , relative to production in the color-octet channel.

There has been little previous work on open charm production in bottomonium decays. In 1978, Fritzsche and Streng calculated the decay rate of  $\Upsilon$  into charm at leading order in  $\alpha_s$  [6]. In 1979, Barbieri, Caffo, and Remiddi calculated the decay rates of the  $P$ -wave bottomonium states into charm at leading order in  $\alpha_s$  under the assumption that the rates could be expressed as products of  $|R'(0)|^2$  and a perturbatively calculable coefficient [7]. In the case of  $\chi_{b0}$  and  $\chi_{b2}$ , the coefficients contained infrared divergences that were expressed in terms of logarithms of the binding energy. However, as we have mentioned, the correct interpretation of the infrared divergences is that they are contained in the probability to find the  $Q\bar{Q}$  pair at a point in a color-octet state. By making use of the NRQCD factorization formalism, one can now carry out rigorous calculations of inclusive charm production from  $\chi_{bJ}$  decays.

In their 1979 paper, Barbieri, Caffo, and Remiddi calculated the invariant mass distribution of the  $c\bar{c}$  pair in  $\chi_{bJ}$  decays. In order to make contact with experiment, one might be tempted to identify this distribution with the invariant mass distribution of pairs of charm hadrons. However that distribution cannot be measured easily because the probability of identifying both charm hadrons is very low. Furthermore, the effects of the hadronization of the charm quark into a charm hadron have a large effect on the distribution. These effects cannot be calculated perturbatively, and they would also be very difficult to measure. A more useful quantity to calculate is the momentum distribution of the charm quark in  $\chi_{bJ}$  decays. This cannot be compared directly with the momentum distribution of the charm hadrons because of the effects of hadronization. However, the effects of hadronization can be determined experimentally by measuring the momentum distribution of charm hadrons in  $e^+e^-$  annihilation.

On the experimental side, the spin-triplet members of two multiplets of  $P$ -wave bottomonium states have been discovered:  $\chi_{bJ}(1P)$  and  $\chi_{bJ}(2P)$ . The only properties of these states that have been measured thus far are their masses and their radiative branching fractions into the  $S$ -wave bottomonium states  $\Upsilon(nS)$ . The total widths of the  $\chi_{bJ}(nP)$  states have not

been measured. Recent runs of the CLEO experiment at the  $\Upsilon(2S)$  and  $\Upsilon(3S)$  resonances have provided new data on the  $\chi_{bJ}(1P)$  and  $\chi_{bJ}(2P)$  states. The  $B$ -factory experiments BABAR and Belle can study the  $\chi_{bJ}(nP)$  states by using data samples of  $\Upsilon(2S)$  and  $\Upsilon(3S)$  provided by initial-state radiation. The Belle experiment has also accumulated data by running directly on the  $\Upsilon(3S)$  state.

In this paper, we study inclusive charm production in  $P$ -wave bottomonium decays. In Sec. II, we present the NRQCD factorization formulas for the annihilation decays of  $P$ -wave bottomonium states, and we discuss the NRQCD matrix elements that appear as long-distance factors in the factorization formulas. In Sec. III, we calculate the charm-quark momentum distribution in decays of the spin-triplet  $P$ -wave states  $\chi_{bJ}$ . We include the color-singlet process  $b\bar{b} \rightarrow c\bar{c}g$ , which has a short-distance coefficient of order  $\alpha_s^3$ , and the color-octet process  $b\bar{b} \rightarrow c\bar{c}$ , which has a short-distance coefficient of order  $\alpha_s^2$ . In Sec. IV, we calculate the inclusive rate into charm by integrating over the charm-quark momentum distribution. In Sec. V, we illustrate the momentum distribution for a charm meson  $D$  by convolving the charm-quark momentum distribution with a fragmentation function for  $c \rightarrow D$  that has been measured in  $e^+e^-$  annihilation. Details of the calculations are presented in appendices.

## II. ANNIHILATION DECAYS OF $P$ -WAVE BOTTOMONIUM

The NRQCD factorization formula expresses the annihilation contribution to the hadronic width of a heavy quarkonium state as an infinite sum of products of short-distance coefficients, which can be calculated as power series in  $\alpha_s$ , and nonperturbative long-distance factors [5]. The long-distance factors can be expressed as expectation values of local four-quark operators  $\mathcal{O}_c(^{2S+1}L_J)$  that are defined in Ref. [5]. These NRQCD matrix elements scale as definite powers of the velocity  $v$  of the heavy quark in the quarkonium rest frame. For each of the  $P$ -wave states, there are only two matrix elements that contribute up to corrections of relative order  $v^2$ :  $\langle \mathcal{O}_1(^3P_J) \rangle_{\chi_{bJ}}$  and  $\langle \mathcal{O}_8(^3S_1) \rangle_{\chi_{bJ}}$  for  $\chi_{bJ}$  and  $\langle \mathcal{O}_1(^1P_1) \rangle_{h_b}$  and  $\langle \mathcal{O}_8(^1S_0) \rangle_{h_b}$  for  $h_b$ . Heavy-quark spin symmetry can be used to reduce all these matrix elements at leading order in  $v$  to two independent matrix elements that we will denote by

$\langle \mathcal{O}_1 \rangle_{\chi_b}$  and  $\langle \mathcal{O}_8 \rangle_{\chi_b}^{(\Lambda)}$ :

$$\langle \mathcal{O}_1 \rangle_{\chi_b} = \langle \mathcal{O}_1(^1P_1) \rangle_{h_b} \approx \langle \mathcal{O}_1(^3P_J) \rangle_{\chi_{bJ}}, \quad (1a)$$

$$\langle \mathcal{O}_8 \rangle_{\chi_b}^{(\Lambda)} = \langle \mathcal{O}_8(^1S_0) \rangle_{h_b}^{(\Lambda)} \approx \langle \mathcal{O}_8(^3S_1) \rangle_{\chi_{bJ}}^{(\Lambda)}. \quad (1b)$$

The superscript  $(\Lambda)$  on  $\langle \mathcal{O}_8 \rangle_{\chi_b}^{(\Lambda)}$  indicates the sensitivity of this matrix element to the NRQCD factorization scale. There is a total of 10 independent matrix elements that contribute through order  $v^2$  [8].

The NRQCD factorization formulas for the annihilation widths of the  $\chi_{bJ}$  at leading order in  $v$  can be expressed as

$$\Gamma[\chi_{bJ} \rightarrow X] = A_J(\Lambda) \frac{\langle \mathcal{O}_1 \rangle_{\chi_b}}{m_b^4} + A_8 \frac{\langle \mathcal{O}_8 \rangle_{\chi_b}^{(\Lambda)}}{m_b^2}, \quad (2)$$

where  $X$  represents all possible states that consist of hadrons lighter than the  $B$  meson, and  $\Lambda$  is the NRQCD factorization scale. An analogous equation holds for the rate  $d\Gamma[\chi_{bJ} \rightarrow X]$  that is differential in the kinematic variables. The short-distance coefficients whose leading terms are order  $\alpha_s^2$  are

$$A_0 = \frac{3C_F}{N_c} \pi \alpha_s^2, \quad (3a)$$

$$A_2 = \frac{4C_F}{5N_c} \pi \alpha_s^2, \quad (3b)$$

$$A_8 = \frac{1}{3} n_f \pi \alpha_s^2, \quad (3c)$$

where  $N_c = 3$  is the number of colors,  $C_F = (N_c^2 - 1)/(2N_c) = 4/3$ ,  $n_f = 4$  is the number of light flavors of quarks, including charm, and the masses of the light quarks have been neglected. The coefficients  $A_0$  and  $A_2$  were first calculated by Barbieri, Gatto, and Kogerler in 1976 [1]. The coefficient  $A_8$  was first calculated for massless quarks in Ref. [5]. The short-distance coefficients whose leading terms are order  $\alpha_s^3$  are

$$A_1(\Lambda) = \frac{C_F \alpha_s^3}{N_c} \left[ \left( \frac{587}{54} - \frac{317}{288} \pi^2 \right) C_A + \left( -\frac{16}{27} - \frac{4}{9} \log \frac{\Lambda}{2m_b} \right) n_f \right], \quad (4)$$

where  $C_A = N_c = 3$ , and, again, the masses of the quarks, including the charm quark, have been neglected. The coefficient  $A_1$  was calculated in Refs. [9, 10]. The coefficients  $A_J(\Lambda)$  depend on  $\Lambda$ , beginning at order  $\alpha_s^3$ , in such a way as to cancel the dependence of the matrix element  $\langle \mathcal{O}_8 \rangle_{\chi_b}^{(\Lambda)}$  on  $\Lambda$ . The next-to-leading-order terms in the coefficients  $A_0$ ,  $A_2$ , and  $A_8$  have been calculated by Petrelli, Cacciari, Greco, Maltoni, and Mangano [9] and by

Huang and Chao [10]. The short-distance coefficients are insensitive to  $m_c$ , the mass of the charm quark. The dependence of the leading terms in  $A_J$  and  $A_8$  on  $m_c$  will be calculated in Sec. IV. The leading correction term in  $A_8$  is proportional to  $\alpha_s^2(m_c/m_b)^4$ . The leading correction terms in  $A_J$  are proportional to  $\alpha_s^3(m_c/m_b)^2$ .

In the NRQCD factorization formula in Eq. (2), the decay rates are summed over all light hadronic states. In most cases, there are no factorization formulas for less inclusive decay rates. An exception is the inclusive charm decay rate. The decay of  $\chi_{bJ}$  into a final state that includes charm hadrons requires the annihilation of the  $b\bar{b}$  pair into partons that include a  $c\bar{c}$  pair. The mass of the charm quark is large enough that the contribution to the short-distance coefficients from  $b\bar{b}$  annihilation into  $c\bar{c}$  pairs may be calculable in perturbation theory. At leading order in  $v$ , the NRQCD factorization formula for the inclusive charm decay rate of  $\chi_{bJ}$  involves the same matrix elements as the completely inclusive annihilation decay rate in Eq. (2):

$$\Gamma[\chi_{bJ} \rightarrow c + X] = A_J^{(c)}(\Lambda) \frac{\langle \mathcal{O}_1 \rangle_{\chi_b}}{m_b^4} + A_8^{(c)} \frac{\langle \mathcal{O}_8 \rangle_{\chi_b}^{(\Lambda)}}{m_b^2}, \quad (5)$$

where  $c + X$  represents all possible states that include a charm hadron. The short-distance coefficients  $A_J^{(c)}$  and  $A_8^{(c)}$  are power series in  $\alpha_s$  whose coefficients are functions of the mass ratio  $m_c/m_b$ . We can deduce the limit as  $m_c \rightarrow 0$  of the leading term in  $A_8^{(c)}$  from the value of  $A_8$  in Eq. (3c):  $A_8^{(c)} \rightarrow (1/3)\pi\alpha_s^2$ . Unlike the coefficients in the fully inclusive factorization formula in Eq. (2), the coefficients  $A_J^{(c)}$  and  $A_8^{(c)}$  in Eq. (5) are sensitive to the charm-quark mass. The leading terms in  $A_J^{(c)}$  and  $A_8^{(c)}$  will be calculated in Sec. IV. We will find that the leading term in  $A_J^{(c)}$ , which is of order  $\alpha_s^3$ , depends logarithmically on  $m_c/m_b$ .

The NRQCD matrix elements in Eqs. (1) can, in principle, be calculated by using lattice simulations of NRQCD. The feasibility of such calculations was first demonstrated by Bodwin, Sinclair, and Kim using quenched lattice NRQCD [11]. The best calculations available to date have been carried out using two dynamical light quarks [12]. After extrapolation to three light-quark flavors [12], the values for the  $1P$  multiplet are

$$\langle \mathcal{O}_1 \rangle_{\chi_b(1P)} = 3.2 \pm 0.7 \text{ GeV}^5, \quad (6a)$$

$$\frac{\langle \mathcal{O}_8 \rangle_{\chi_b(1P)}^{(\Lambda)}}{\langle \mathcal{O}_1 \rangle_{\chi_b(1P)}} = 0.0021 \pm 0.0007 \text{ GeV}^{-2}. \quad (6b)$$

We have estimated the errors for the three-flavor case by treating the systematic errors from the quenched and two-flavor calculations as 100% correlated, treating the statistical errors as

uncorrelated, and adding the resulting systematic and statistical errors for the three-flavor case in quadrature. The matrix element  $\langle \mathcal{O}_8 \rangle_{\chi_b(1P)}^{(\Lambda)}$  in Eq. (6b) was computed at  $\Lambda = 4.3$  GeV.

The color-singlet matrix elements can also be estimated by using potential models for heavy quarkonium:

$$\langle \mathcal{O}_1 \rangle_{\chi_b(nP)} \approx \frac{3N_c}{2\pi} |R'_{nP}(0)|^2, \quad (7)$$

where  $N_c = 3$  is the number of colors and  $R_{nP}(r)$  is the radial wave function for the  $nP$  multiplet. The values of  $|R'_{nP}(0)|^2$  for four potential models have been tabulated in Ref. [13]. Using the value of  $|R'_{nP}(0)|^2$  for the Buchmüller-Tye potential, we obtain

$$\langle \mathcal{O}_1 \rangle_{\chi_b(1P)} \approx 2.03 \text{ GeV}^5, \quad (8a)$$

$$\langle \mathcal{O}_1 \rangle_{\chi_b(2P)} \approx 2.37 \text{ GeV}^5. \quad (8b)$$

The values of  $\langle \mathcal{O}_1 \rangle_{\chi_b(nP)}$  from the four potential models in Ref. [13] range from those in Eqs. (8) to those for the Cornell potential, which are about 50% larger. In the case of  $S$ -wave states, there has been recent progress in determining the color-singlet NRQCD matrix element from potential models [14]. The value of the radial wavefunction at the origin  $|R_{1S}(0)|^2$  of the  $\Upsilon(1S)$  that follows from these methods agrees most closely with that from the Buchmüller-Tye potential.

With the choice of normalization of the operators in Ref. [5], the color-octet matrix element  $\langle \mathcal{O}_8 \rangle_{\chi_b}$  can be interpreted intuitively as the probability density at the origin for the  $b\bar{b}$  pair to be in a color-octet state. One can obtain an order-of-magnitude estimate of a lower bound on the quantity  $\langle \mathcal{O}_8 \rangle_{\chi_b}$  by using the renormalization properties of the operators [5]. The operator  $\mathcal{O}_8$  depends on a renormalization scale  $\Lambda$ , and it mixes under renormalization with  $\mathcal{O}_1$ . The solution to the renormalization group equation at leading order in  $\alpha_s$  is [5]

$$\langle \mathcal{O}_8 \rangle_{\chi_b}^{(m_b)} = \langle \mathcal{O}_8 \rangle_{\chi_b}^{(\Lambda)} + \frac{4C_F}{3N_c\beta_0} \log \left( \frac{\alpha_s(\Lambda)}{\alpha_s(m_b)} \right) \frac{\langle \mathcal{O}_1 \rangle_{\chi_b}}{m_b^2}, \quad (9)$$

where  $\beta_0 = (11N_c - 2n_f)/6 = 25/6$  is the first coefficient in the beta function for QCD with  $n_f = 4$  flavors of light quarks. The second term on the right side of Eq. (9) has a physical interpretation as a correction from gluon radiation that arises from gluon energies between  $\Lambda$  and  $m_b$ . Since  $m_b v$  is the typical momentum scale in a quarkonium state, we choose  $\Lambda = m_b v$ . Unless there is a near cancellation between the two terms in Eq. (9) for  $\Lambda = m_b v$ , the matrix element  $\langle \mathcal{O}_8 \rangle_{\chi_b}^{(m_b)}$  should either be comparable to or larger than the second term

on the right side. This gives us an order-of-magnitude estimate of a lower bound on the matrix element:

$$\langle \mathcal{O}_8 \rangle_{\chi_b}^{(m_b)} \gtrsim \frac{32}{225} \log \left( \frac{\alpha_s(m_b v)}{\alpha_s(m_b)} \right) \frac{\langle \mathcal{O}_1 \rangle_{\chi_b}}{m_b^2}. \quad (10)$$

Since the one-loop bottom-quark pole mass is  $m_b^{(\text{pole})} \approx 4.6$  GeV, we set  $m_b = 4.6$  GeV and  $m_b v = 1.5$  GeV. Then our estimated lower bound on the dimensionless ratio of the matrix elements

$$\rho_8 = m_b^2 \langle \mathcal{O}_8 \rangle_{\chi_b}^{(m_b)} / \langle \mathcal{O}_1 \rangle_{\chi_b} \quad (11)$$

is  $\rho_8 \gtrsim 0.068$ . In comparison, the lattice results in Eq. (6), taken with  $m_b = 4.6$  GeV, give  $\rho_8 = 0.044 \pm 0.015$ . Given the errors, this result is compatible with the estimated lower bound from Eq. (10).

In NRQCD, there is no general relation between the matrix elements  $\langle \mathcal{O}_1 \rangle_{\chi_b}$  and  $\langle \mathcal{O}_8 \rangle_{\chi_b}^{(m_b)}$  for different  $P$ -wave multiplets. However, if the scale  $m_b v^2$  is below the QCD scale  $\Lambda_{\text{QCD}}$ , then the ratio  $\rho_8$  in Eq. (11) is the same for all the  $P$ -wave multiplets [15].

### III. CHARM QUARK PRODUCTION IN $\chi_b$ DECAY

#### A. Perturbative matching

The coefficients in the NRQCD factorization formula for inclusive charm production in Eq. (5) are short-distance quantities that are insensitive to the long-distance behavior of the external  $b\bar{b}$  states. This implies that the short-distance coefficients can be computed in perturbation theory. It also implies that, for purposes of computing the short-distance coefficients, we can replace the external  $b\bar{b}$  hadronic states in the factorization formula with perturbative  $b\bar{b}$  states. We compute the short-distance coefficients by matching the perturbative expressions for the  $b\bar{b}$  annihilation rates in full QCD with the corresponding perturbative NRQCD factorization expressions for the annihilation rates. The perturbative analog of the NRQCD factorization formula in Eq. (5) for the annihilation rates of appropriate  $b\bar{b}$  states is

$$d\Gamma[b\bar{b} \rightarrow c + X] = \sum_{J=0}^2 dA_J^{(c)}(\Lambda) \frac{\langle \mathcal{O}_1(^3P_J) \rangle_{b\bar{b}}}{m_b^4} + dA_8^{(c)} \frac{\langle \mathcal{O}_8(^3S_1) \rangle_{b\bar{b}}^{(\Lambda)}}{m_b^2}. \quad (12)$$

We have written the factorization formula in differential form so that we can consider distributions in kinematic variables associated with the charm quark. We can determine the

four short-distance coefficients  $dA_J^{(c)}$  and  $dA_8^{(c)}$  by (i) calculating the annihilation rate in perturbative QCD for a  $b\bar{b}$  pair in four appropriate independent  $b\bar{b}$  states, (ii) calculating the NRQCD matrix elements for each of those four states using perturbative NRQCD, and then (iii) solving the linear set of equations for the coefficients.

We wish to calculate the short-distance coefficients at leading order in  $\alpha_s$ , which is order  $\alpha_s^2$  for  $A_8^{(c)}$  and order  $\alpha_s^3$  for  $A_J^{(c)}$ . At this order, we must take into account the renormalization of the NRQCD matrix element  $\langle \mathcal{O}_8(^3S_1) \rangle_{b\bar{b}}$ . We regularize the NRQCD matrix element by using dimensional regularization in  $d = 4 - 2\epsilon$  space-time dimensions, and we define the renormalized NRQCD matrix element by using the modified minimal subtraction ( $\overline{\text{MS}}$ ) prescription. The relation between the bare operator  $\mathcal{O}_8(^3S_1)$  and the renormalized operator  $\mathcal{O}_8(^3S_1)^{(\Lambda)}$  with NRQCD factorization scale  $\Lambda$  is [5, 9]

$$\mathcal{O}_8(^3S_1) = \mathcal{O}_8(^3S_1)^{(\Lambda)} + \frac{(4\pi e^{-\gamma})^\epsilon}{\epsilon_{\text{UV}}} \frac{2C_F\alpha_s}{3\pi N_c m_b^2} \sum_{J=0}^2 \mathcal{O}_1(^3P_J) + \dots \quad (13)$$

The subscript UV indicates that the pole in  $\epsilon$  is associated with an ultraviolet divergence. We have shown explicitly only those terms that contribute through order  $\alpha_s$  and at leading order in  $v$  to the expectation values in a color-singlet  $P$ -wave  $b\bar{b}$  state or in a color-octet  $S$ -wave  $b\bar{b}$  state.

The perturbative matrix elements of the NRQCD operators regularized with dimensional regularization are particularly simple if we also use dimensional regularization to regularize infrared divergences and we expand the matrix elements in powers of the relative momentum  $\mathbf{q}$  of the  $b$  and  $\bar{b}$ . In this case, all loop corrections to the regulated matrix element vanish because there is no scale for the dimensionally regularized integrals. In particular, the ultraviolet poles in  $\epsilon$  cancel the infrared poles in  $\epsilon$ . Thus, we have

$$\langle \mathcal{O}_8(^3S_1) \rangle_{b\bar{b}}^{(\text{reg})} = \langle \mathcal{O}_8(^3S_1) \rangle_{b\bar{b}}^{(\text{tree})}, \quad (14)$$

where  $\langle \mathcal{O}_8(^3S_1) \rangle_{b\bar{b}}^{(\text{reg})}$  is the matrix element of the bare NRQCD operator with both infrared and ultraviolet divergences dimensionally regulated, and  $\langle \mathcal{O}_8(^3S_1) \rangle_{b\bar{b}}^{(\text{tree})}$  is the tree-level approximation to the matrix element of the bare NRQCD operator. If we take the expectation value of Eq. (13) in a  $b\bar{b}$  state, dimensionally regulating both UV and IR divergences, and substitute (14), we find that

$$\langle \mathcal{O}_8(^3S_1) \rangle_{b\bar{b}}^{(\Lambda)} = \langle \mathcal{O}_8(^3S_1) \rangle_{b\bar{b}}^{(\text{tree})} - \frac{(4\pi e^{-\gamma})^\epsilon}{\epsilon_{\text{IR}}} \frac{2C_F\alpha_s}{3\pi N_c m_b^2} \sum_{J=0}^2 \langle \mathcal{O}_1(^3P_J) \rangle_{b\bar{b}} + \dots \quad (15)$$

The subscript IR indicates that the pole in  $\epsilon$  is now associated with an infrared divergence.

To determine the four short-distance coefficients  $A_J^{(c)}$  and  $A_8^{(c)}$  in Eq. (5), we must calculate the annihilation rate for four appropriate  $b\bar{b}$  states using perturbative QCD. A convenient choice for these states consists of a  $b\bar{b}$  pair in a color-octet  $^3S_1$  state, which we denote by  $b\bar{b}_8(^3S_1)$ , and a  $b\bar{b}$  pair in each of the three color-singlet  $^3P_J$  states, which we denote by  $b\bar{b}_1(^3P_J)$ . For these states, the factorization formula in Eq. (12) reduces at leading order in  $\alpha_s$  and at leading order in  $v$  to

$$d\Gamma[b\bar{b}_8(^3S_1) \rightarrow c + X] = dA_8^{(c)} \frac{\langle \mathcal{O}_8(^3S_1) \rangle_{b\bar{b}_8(^3S_1)}^{(\Lambda)}}{m_b^2}, \quad (16a)$$

$$d\Gamma[b\bar{b}_1(^3P_J) \rightarrow c + X] = dA_J^{(c)}(\Lambda) \frac{\langle \mathcal{O}_1(^3P_J) \rangle_{b\bar{b}_1(^3P_J)}^{(\Lambda)}}{m_b^4} + dA_8^{(c)} \frac{\langle \mathcal{O}_8(^3S_1) \rangle_{b\bar{b}_1(^3P_J)}^{(\Lambda)}}{m_b^2}. \quad (16b)$$

In Eq. (16a), the term involving the color-singlet operator does not contribute because it is of higher order in  $\alpha_s$ . In Eq. (16b), the color-octet matrix element  $\langle \mathcal{O}_8(^3S_1) \rangle_{b\bar{b}_1(^3P_J)}^{(\Lambda)}$  can be simplified by using the fact that the tree-level term in Eq. (15) does not contribute. The factorization formula in Eq. (16b) can then be reduced to

$$d\Gamma[b\bar{b}_1(^3P_J) \rightarrow c + X] = \left( dA_J^{(c)}(\Lambda) - \frac{(4\pi e^{-\gamma})^\epsilon 2C_F\alpha_s}{\epsilon_{\text{IR}} 3\pi N_c} dA_8^{(c)} \right) \frac{\langle \mathcal{O}_1(^3P_J) \rangle_{b\bar{b}_1(^3P_J)}^{(\Lambda)}}{m_b^4}. \quad (17)$$

Eqs. (16a) and (17) can be solved to obtain the short-distance coefficients  $dA_8^{(c)}$  and  $dA_J^{(c)}$  in terms of the perturbative decay rates  $d\Gamma[b\bar{b}_8(^3S_1) \rightarrow c + X]$  and  $d\Gamma[b\bar{b}_1(^3P_J) \rightarrow c + X]$  and the perturbative matrix elements  $\langle \mathcal{O}_8(^3S_1) \rangle_{b\bar{b}_8(^3S_1)}^{(\Lambda)}$  and  $\langle \mathcal{O}_1(^3P_J) \rangle_{b\bar{b}_1(^3P_J)}^{(\Lambda)}$ . At the order in  $\alpha_s$  of the present calculation, the perturbative matrix elements can be computed at tree level. In the next three subsections, we compute the required perturbative decay rates and perturbative matrix elements. As we will see,  $d\Gamma[b\bar{b}_1(^3P_J) \rightarrow c + X]$  contains an infrared divergence that is canceled by the explicit infrared divergence in the second term on the right side of Eq. (17). The short-distance coefficients are then infrared finite, as expected.

## B. Amplitudes for $b\bar{b}$ annihilation into charm

The momenta of the  $b$  and  $\bar{b}$  that annihilate to produce charm can be expressed as

$$p = \frac{1}{2}P + q, \quad (18a)$$

$$\bar{p} = \frac{1}{2}P - q, \quad (18b)$$

where  $P$  and  $q$  are the total and relative momenta of the  $b\bar{b}$  pair. In the rest frame of the  $b\bar{b}$  pair, the explicit momenta are  $P = (2E_b, 0)$  and  $q = (0, \mathbf{q})$ , where  $E_b = \sqrt{m_b^2 + \mathbf{q}^2}$  and  $m_b$  is the mass of the bottom quark. An annihilation amplitude can be expressed in the form

$$\bar{v}(\bar{p})\mathcal{A}u(p) = \text{Tr}[\mathcal{A}u(p)\bar{v}(\bar{p})], \quad (19)$$

where  $\mathcal{A}$  is a matrix that acts on spinors with both Dirac and color indices. The amplitude in Eq. (19) can be projected into a particular spin and color channel by replacing  $u(p)\bar{v}(\bar{p})$  with a projection matrix. The color projectors  $\pi_1$  and  $\pi_8^a$  onto a color-singlet state and onto a color-octet state with color index  $a$  are

$$\pi_1 = \frac{1}{\sqrt{N_c}}\mathbb{1}, \quad (20a)$$

$$\pi_8^a = \sqrt{2}T^a, \quad (20b)$$

where  $\mathbb{1}$  is the  $3 \times 3$  unit matrix and  $T^a$  is a generator of the fundamental representation of SU(3). The color projectors are normalized so that  $\text{Tr}[\pi_1\pi_1^\dagger]=1$  and  $\text{Tr}[\pi_8^a\pi_8^{b\dagger}] = \delta^{ab}$ . The projector onto a spin-triplet state with four-momentum  $P^\mu$ , rest energy  $\sqrt{P^2} = 2E_b$ , and spin polarization vector  $\epsilon_S$  satisfying  $P \cdot \epsilon_S = 0$  is  $\epsilon_{S\mu}\Pi_3^\mu$  [16–18], where

$$\Pi_3^\mu = \frac{-1}{4\sqrt{2}E_b(E_b + m_b)}(\not{p} + m_b)(\not{P} + 2E_b)\gamma^\mu(\not{p} - m_b). \quad (21)$$

The spin projector is normalized so that

$$\text{Tr}[(\epsilon_S \cdot \Pi_3)(\epsilon_S \cdot \Pi_3)^\dagger] = 4p_0\bar{p}_0. \quad (22)$$

At leading order in  $v$ , the amplitude for the annihilation of a  $b\bar{b}$  pair in a color-octet spin-triplet  $S$ -wave state with spin polarization vector  $\epsilon_S$  is  $\epsilon_{S\mu}\mathcal{A}_8^{a\mu}$ , where

$$\mathcal{A}_8^{a\mu} = \text{Tr}[\mathcal{A}(\Pi_3^\mu \otimes \pi_8^a)] \Big|_{q=0}. \quad (23)$$

The leading color-octet mechanism for producing charm in  $b\bar{b}$  annihilation is via the process  $b\bar{b} \rightarrow c\bar{c}$ , whose rate is of order  $\alpha_s^2$ . The matrix  $\mathcal{A}$  for the process  $b(p)\bar{b}(\bar{p}) \rightarrow c(p_1)\bar{c}(p_2)$  is

$$\mathcal{A}[b\bar{b} \rightarrow c\bar{c}] = \frac{-g_s^2}{(p_1 + p_2)^2}\bar{u}(p_1)T^b\gamma_\nu v(p_2) [T^b\gamma^\nu]. \quad (24)$$

Using Eq. (23), we find that the coefficient of  $\epsilon_{S\mu}$  in the annihilation amplitude is

$$\mathcal{A}_8^{a\mu} = \frac{g_s^2}{2m_b}\bar{u}(p_1)T^a\gamma^\mu v(p_2), \quad (25)$$

where we have omitted terms proportional to  $P^\mu$  because  $P \cdot \epsilon_S = 0$ .

At leading order in the relative velocity  $v$  of the  $b$  or  $\bar{b}$  in the quarkonium rest frame, the amplitude for the annihilation of a  $b\bar{b}$  pair in a color-singlet spin-triplet  $P$ -wave state with spin polarization vector  $\epsilon_S$  and orbital-angular-momentum polarization vector  $\epsilon_L$  is  $\epsilon_{L\nu}\epsilon_{S\mu}\mathcal{A}_1^{\mu\nu}$ , where

$$\mathcal{A}_1^{\mu\nu} = \frac{\partial}{\partial q_\nu} \text{Tr}[\mathcal{A}(\Pi_3^\mu \otimes \pi_1)]|_{q=0}. \quad (26)$$

The leading color-singlet mechanism for producing charm in  $b\bar{b}$  annihilation is the process  $b\bar{b} \rightarrow c\bar{c}g$ , whose rate is of order  $\alpha_s^3$ . The matrix  $\mathcal{A}$  for the process  $b(p)\bar{b}(\bar{p}) \rightarrow c(p_1)\bar{c}(p_2)g(p_3)$  is

$$\begin{aligned} \mathcal{A}[b\bar{b} \rightarrow c\bar{c}g] &= \frac{-g_s^3}{(p_1 + p_2)^2} \bar{u}(p_1) T^a \gamma_\lambda v(p_2) \epsilon_\sigma^{b*}(p_3) \\ &\quad \times [T^a T^b \gamma^\lambda \Lambda(p - p_3) \gamma^\sigma + T^b T^a \gamma^\sigma \Lambda(-\bar{p} + p_3) \gamma^\lambda], \end{aligned} \quad (27)$$

where  $\Lambda(k)$  is defined by

$$\Lambda(k) = \frac{\not{k} + m_b}{k^2 - m_b^2}. \quad (28)$$

Using Eq. (26), we find that

$$\begin{aligned} \mathcal{A}_1^{\mu\nu} &= \frac{-g_s^3}{2\sqrt{N_c}(P - p_3)^2} \bar{u}(p_1) T^a \gamma_\lambda v(p_2) \epsilon_\sigma^{a*}(p_3) \\ &\quad \times \frac{\partial}{\partial q_\nu} \text{Tr}\left\{[\gamma^\lambda \Lambda(p - p_3) \gamma^\sigma + \gamma^\sigma \Lambda(-\bar{p} + p_3) \gamma^\lambda] \Pi_3^\mu\right\}|_{q=0}. \end{aligned} \quad (29)$$

### C. Color-octet short-distance coefficient

We proceed to calculate the differential coefficient  $dA_8^{(c)}$  of the color-octet term in the NRQCD factorization formula. We use the perturbative factorization formula in Eq. (16a), which requires calculating the annihilation rate of a  $b\bar{b}$  pair in a color-octet  $^3S_1$  state. The resulting expression for  $dA_8^{(c)}$  will also be needed in the determination of the coefficients  $dA_J^{(c)}$  that makes use of the perturbative factorization formula in Eq. (17). In that equation,  $dA_8^{(c)}$  is multiplied by a pole in  $\epsilon$ . It is therefore necessary to calculate  $dA_8^{(c)}$  in  $d = 4 - 2\epsilon$  space-time dimensions.

The differential annihilation rate of a color-octet  $^3S_1$   $b\bar{b}$  state into charm through the color-octet process  $b\bar{b} \rightarrow c\bar{c}$  can be expressed in the form

$$d\Gamma[b\bar{b}_8(^3S_1) \rightarrow c + X] = \left( \frac{1}{d-1} I_{\mu\alpha} \sum_{c\bar{c}} \mathcal{A}_8^{a\mu} \mathcal{A}_8^{a\alpha*} \right) d\Phi_2, \quad (30)$$

where  $\mathcal{A}_8^{a\mu}$  is the amplitude in Eq. (25),  $d\Phi_2$  is the differential 2-body phase space for  $c\bar{c}$ , and  $I^{\mu\nu}$  is the projection tensor for spin 1:

$$I^{\mu\nu} = -g^{\mu\nu} + \frac{P^\mu P^\nu}{P^2}. \quad (31)$$

The factor of  $1/(d-1)$  in Eq. (30) comes from averaging over the spin states of the  $b\bar{b}$  pair. The explicit sum in Eq. (30) is over the color and spin states of the  $c$  and  $\bar{c}$ . The evaluation of that sum gives

$$I_{\mu\alpha} \sum_{c\bar{c}} \mathcal{A}_8^{a\mu} \mathcal{A}_8^{a\alpha*} = (4\pi\alpha_s\Lambda^{2\epsilon})^2 (N_c^2 - 1) (d - 2 + r), \quad (32)$$

where  $g_s^2 = 4\pi\alpha_s\Lambda^{2\epsilon}$  and  $\Lambda$  is the scale associated with dimensional regularization. In our calculation,  $\Lambda$  becomes the NRQCD factorization scale. We have set  $E_b \rightarrow m_b$  in  $I^{\mu\nu}$  for consistency with the prescription for  $\mathcal{A}_8^{a\mu}$  in Eq. (23), which involved expanding to leading order in  $v$ .

We wish to obtain an expression for the coefficient that is differential in the energy of the charm quark. We therefore integrate over the entire 2-body phase space, except for  $E_1$ , the energy of the charm quark in the  $b\bar{b}$  rest frame. In the center-of-momentum frame, the differential 2-body phase space in  $d = 4 - 2\epsilon$  space-time dimensions reduces to

$$d\Phi_2 = c_2(\epsilon) \frac{|\mathbf{p}_1|^{1-2\epsilon}}{8\pi E_b} \delta(E_1 - E_b) dE_1, \quad (33)$$

where  $|\mathbf{p}_1| = (E_1^2 - m_c^2)^{1/2}$  is the magnitude of the three-momentum of the charm quark and  $2E_b$  is the energy of the  $b\bar{b}$  pair. The dimensionless coefficient  $c_2(\epsilon)$ , which reduces to 1 as  $\epsilon \rightarrow 0$ , is defined by

$$c_2(\epsilon) = (4\pi)^\epsilon \frac{\Gamma(\frac{3}{2})}{\Gamma(\frac{3}{2} - \epsilon)}. \quad (34)$$

It is useful to express the differential phase space in terms of an energy fraction  $x_1$  for the charm quark defined by

$$x_1 = E_1/E_b. \quad (35)$$

There is some ambiguity in the choice of  $E_b$ . The choice  $E_b = M_{\chi_{bJ}}/2$  gives the correct kinematic limits on the energy of the charm quark. However, we choose  $E_b = m_b$  in order to maintain consistency with the nonrelativistic approximation that we used in computing  $\mathcal{A}_8^{a\mu}$  in Eq. (23). The expression for the differential phase space then reduces to

$$d\Phi_2 = \frac{c_2(\epsilon)}{[(1-r)m_b^2]^\epsilon} \frac{\sqrt{1-r}}{8\pi} \delta(1-x_1) dx_1, \quad (36)$$

where  $r$  is the square of the ratio of the charm- and bottom-quark masses:

$$r = m_c^2/m_b^2. \quad (37)$$

Inserting the differential phase space in Eq. (36) into Eq. (30) and using Eq. (32), we find that the expression for the differential annihilation rate reduces to

$$d\Gamma[b\bar{b}_8(^3S_1) \rightarrow c + X] = \frac{c_2(\epsilon)\Lambda^{4\epsilon}}{[(1-r)m_b^2]^\epsilon} \times \frac{2(N_c^2 - 1)(d - 2 + r)\sqrt{1-r}\pi\alpha_s^2}{d - 1} \delta(1 - x_1)dx_1. \quad (38)$$

To complete the matching calculation of the coefficient  $dA_8^{(c)}$ , we need to evaluate the NRQCD matrix element on the right side of the factorization formula in Eq. (16a). The  $b\bar{b}$  states have the standard relativistic normalizations. At leading order in the nonrelativistic expansion, the matrix element is therefore

$$\langle \mathcal{O}_8(^3S_1) \rangle_{b\bar{b}_8(^3S_1)} = 4(N_c^2 - 1)m_b^2. \quad (39)$$

Inserting Eqs. (38) and (39) into Eq. (16a), we find that the differential coefficient  $dA_8^{(c)}$  in  $d$  dimensions is

$$dA_8^{(c)} = \frac{c_2(\epsilon)\Lambda^{4\epsilon}}{[(1-r)m_b^2]^\epsilon} \times \frac{(d - 2 + r)\sqrt{1-r}}{2(d - 1)} \pi\alpha_s^2 \delta(1 - x_1)dx_1. \quad (40)$$

Upon setting  $\epsilon = 0$ , we find that the differential coefficient with respect to the energy fraction of the charm quark reduces to

$$\frac{dA_8^{(c)}}{dx_1} = \frac{(1 + r/2)\sqrt{1-r}}{3} \pi\alpha_s^2 \delta(1 - x_1). \quad (41)$$

#### D. Color-singlet short-distance coefficients

We next calculate the differential coefficients  $dA_J^{(c)}$  of the color-singlet terms in the NRQCD factorization formula. We use the perturbative factorization formula in Eq. (17), which requires calculating the annihilation rate of a  $b\bar{b}$  pair in a color-singlet  $^3P_J$  state for  $J = 0, 1$ , and  $2$ . This annihilation rate is infrared divergent at leading order in  $\alpha_s$ . We use dimensional regularization in  $d = 4 - 2\epsilon$  space-time dimensions to regularize the infrared divergence.

The differential annihilation rate of a color-singlet  $^3P_J$   $b\bar{b}$  state into charm through the color-singlet process  $b\bar{b} \rightarrow c\bar{c}g$  can be expressed in the form

$$d\Gamma[b\bar{b}_1(^3P_J) \rightarrow c + X] = \left( \frac{1}{S_J(d)} K_{\mu\nu;\alpha\beta}^J \sum_{c\bar{c}g} \mathcal{A}_1^{\mu\nu} \mathcal{A}_1^{*\alpha\beta} \right) d\Phi_3, \quad (42)$$

where  $\mathcal{A}_1^{\mu\nu}$  is the amplitude in Eq. (29),  $d\Phi_3$  is the differential three-body phase space for  $c\bar{c}g$ , and the  $K_{\mu\nu;\alpha\beta}^J$  are the projection tensors for total angular momentum  $J$ . In  $d$  space-time dimensions, these projectors are [9]

$$K_{\mu\nu;\alpha\beta}^0 = \frac{1}{d-1} I^{\mu\nu} I^{\alpha\beta}, \quad (43a)$$

$$K_{\mu\nu;\alpha\beta}^1 = \frac{1}{2} (I^{\mu\alpha} I^{\nu\beta} - I^{\mu\beta} I^{\nu\alpha}), \quad (43b)$$

$$K_{\mu\nu;\alpha\beta}^2 = \frac{1}{2} (I^{\mu\alpha} I^{\nu\beta} + I^{\mu\beta} I^{\nu\alpha}) - \frac{1}{d-1} I^{\mu\nu} I^{\alpha\beta}, \quad (43c)$$

where  $I^{\mu\nu}$  is given in Eq. (31). For  $J = 0, 1$ , and  $2$ ,  $K_{\mu\nu;\alpha\beta}^J$  projects the tensor  $\mathcal{A}_1^{\mu\nu}$  onto its trace, its antisymmetric part, and its traceless symmetric part, respectively. The factor of  $S_J(d)$  in Eq. (42) comes from averaging over the angular momentum states of the  $b\bar{b}$  pair. The spin- $J$  multiplicities in  $d$  dimensions are

$$S_0(d) = K_{\mu\nu;\alpha\beta}^0 K^{0\mu\nu;\alpha\beta} = 1, \quad (44a)$$

$$S_1(d) = K_{\mu\nu;\alpha\beta}^1 K^{1\mu\nu;\alpha\beta} = \frac{1}{2}(d-1)(d-2), \quad (44b)$$

$$S_2(d) = K_{\mu\nu;\alpha\beta}^2 K^{2\mu\nu;\alpha\beta} = \frac{1}{2}(d+1)(d-2). \quad (44c)$$

The explicit sum in Eq. (42) is over the color and spin states of the  $c$ ,  $\bar{c}$ , and  $g$ . In the expression for the amplitude  $\mathcal{A}_1^{\mu\nu}$  in Eq. (27), the only factors that depend on the spins and colors of the  $c\bar{c}g$  are  $\bar{u}(p_1)$ ,  $v(p_2)$ , and  $\epsilon_{\sigma}^{a*}(p_3)$ . The sum over the spins and colors of the  $c\bar{c}g$  are

$$\begin{aligned} \sum_{c\bar{c}g} \bar{u}(p_1) T^a \gamma_{\lambda} v(p_2) \epsilon_{\sigma}^{a*}(p_3) [\bar{u}(p_1) T^b \gamma_{\rho} v(p_2) \epsilon_{\tau}^{b*}(p_3)]^* \\ = -\frac{N_c^2 - 1}{2} g_{\sigma\tau} \text{Tr}[(\not{p}_1 + m_c) \gamma_{\lambda} (\not{p}_2 - m_c) \gamma_{\rho}]. \end{aligned} \quad (45)$$

We have omitted terms from the sum over gluon spins that are proportional to  $p_{3\sigma}$  or  $p_{3\tau}$ , because they give zero when they are contracted with the trace in Eq. (29) or its complex conjugate. After evaluating the Dirac traces in Eq. (45) and in Eq. (29), we reduce the contracted tensors in the differential decay rate in Eq. (42) to complicated functions of Lorentz scalars, which we will report later in this section.

We wish to obtain expressions for the coefficients  $A_J^{(c)}$  that are differential in the momentum of the charm quark. We must therefore integrate over the entire three-body phase space, except for the energy  $E_1$  of the charm quark in the  $b\bar{b}$  rest frame. The differential three-body phase space in the center-of-momentum frame in  $d = 4 - 2\epsilon$  space-time dimensions is

computed in Appendix A:

$$d\Phi_3 = \frac{(4\pi)^{2\epsilon}}{\Gamma(2-2\epsilon)} \delta(E_1 + E_2 + E_3 - 2E_b) \frac{dE_1 dE_2 dE_3}{32\pi^3 [-\lambda(\mathbf{p}_1^2, \mathbf{p}_2^2, \mathbf{p}_3^2)]^\epsilon}, \quad (46)$$

where  $\lambda(x, y, z) = x^2 + y^2 + z^2 - 2(xy + yz + zx)$  and  $|\mathbf{p}_i| = (E_i^2 - m_i^2)^{1/2}$  is the magnitude of the three-momentum of particle  $i$ . The physical region of  $E_1$ ,  $E_2$ , and  $E_3$  is determined by the delta function and by the condition  $-\lambda(\mathbf{p}_1^2, \mathbf{p}_2^2, \mathbf{p}_3^2) \geq 0$ . The physical region can be determined from the expression

$$-\lambda(\mathbf{p}_1^2, \mathbf{p}_2^2, \mathbf{p}_3^2) = (|\mathbf{p}_1| + |\mathbf{p}_2| + |\mathbf{p}_3|)(|\mathbf{p}_1| + |\mathbf{p}_2| - |\mathbf{p}_3|)(|\mathbf{p}_2| + |\mathbf{p}_3| - |\mathbf{p}_1|)(|\mathbf{p}_3| + |\mathbf{p}_1| - |\mathbf{p}_2|). \quad (47)$$

We let the energies of the  $c$ ,  $\bar{c}$ , and  $g$  be  $E_1$ ,  $E_2$ , and  $E_3$ , respectively. It is convenient to introduce dimensionless energy variables  $x_i$  defined by

$$x_i = E_i/E_b. \quad (48)$$

We can use the delta function in Eq. (46) to integrate over  $x_2$ . If we set  $E_b = m_b$ , then the differential phase space for  $c\bar{c}g$  reduces to

$$d\Phi_3 = \frac{c_3(\epsilon)}{[(x_1^2 - r)x_3^2(1 - \cos^2 \theta_{13})m_b^4]^\epsilon} \frac{m_b^2}{32\pi^3} dx_1 dx_3, \quad (49)$$

where  $c_3(\epsilon)$  is defined by

$$c_3(\epsilon) = \frac{(4\pi)^{2\epsilon} \Gamma(\frac{3}{2})}{\Gamma(1-\epsilon)\Gamma(\frac{3}{2}-\epsilon)} = \frac{(2\pi)^{2\epsilon}}{\Gamma(2-2\epsilon)}, \quad (50)$$

and  $\theta_{13}$  is the angle between the momenta  $p_1$  and  $p_3$ :

$$\sin^2 \theta_{13} = -\lambda(\mathbf{p}_1^2, \mathbf{p}_2^2, \mathbf{p}_3^2)/(4\mathbf{p}_1^2 \mathbf{p}_3^2). \quad (51)$$

The ranges of the variables  $x_1$  and  $x_3$  are given by

$$\sqrt{r} \leq x_1 \leq 1, \quad (52a)$$

$$x_3^- \leq x_3 \leq x_3^+, \quad (52b)$$

where the endpoints of the  $x_3$  integral are

$$x_3^\pm = \frac{2(1-x_1)}{2-x_1 \mp \sqrt{x_1^2 - r}}. \quad (53)$$

After integrating over the energy fractions of the  $\bar{c}$  and  $g$ , we find that the differential annihilation rate in Eq. (42) reduces to

$$d\Gamma[b\bar{b}_1(^3P_J) \rightarrow c + X] = \frac{8C_F\alpha_s^3\Lambda^{6\epsilon}}{m_b^2} \left[ c_3(\epsilon)m_b^{-4\epsilon} \hat{\Gamma}_{\text{div}}^J(x_1) + \hat{\Gamma}_{\text{fin}}^J(x_1) \right] dx_1, \quad (54)$$

where the coefficient  $c_3(\epsilon)$  is defined in Eq. (50). The dimensionless functions  $\hat{\Gamma}_{\text{div}}^J(x_1)$  are defined by

$$\hat{\Gamma}_{\text{div}}^0(x_1) = \frac{(d-2+r)I_0(x_1) - 4[I_1(x_1) - I_2(x_1)]}{(d-1)(x_1^2 - r)^\epsilon}, \quad (55a)$$

$$\hat{\Gamma}_{\text{div}}^1(x_1) = \frac{(d-3)(d-2+r)I_0(x_1) + 4[I_1(x_1) - I_2(x_1)]}{(d-1)(d-2)(x_1^2 - r)^\epsilon}, \quad (55b)$$

$$\hat{\Gamma}_{\text{div}}^2(x_1) = \frac{(d^2 - 2d - 1)(d-2+r)I_0(x_1) - 4(d-3)[I_1(x_1) - I_2(x_1)]}{(d-1)(d+1)(d-2)(x_1^2 - r)^\epsilon}, \quad (55c)$$

where the functions  $I_n(x_1)$  are integrals over  $x_3$ :

$$I_n(x_1) = \int_{x_3^-}^{x_3^+} dx_3 \frac{(1-x_1)^n}{x_3^{n+2+2\epsilon}(1-\cos^2\theta_{13})^\epsilon}. \quad (56)$$

These integrals, which are logarithmically infrared divergent, are evaluated analytically in Appendix B. They can be expressed in terms of two distributions that are singular at  $x_1 = 1$ : the Dirac delta function  $\delta(1-x_1)$  and a distribution  $[1/(1-x_1)]_{\sqrt{r}}$  that is defined by

$$\int_x^1 g(x_1)[f(x_1)]_{\sqrt{r}} dx_1 \equiv \int_x^1 [g(x_1) - g(1)]f(x_1)dx_1 - g(1) \int_{\sqrt{r}}^x f(x_1)dx_1 \quad (57)$$

for any  $x$  in the interval  $\sqrt{r} \leq x < 1$  and any smooth function  $g(x_1)$ . The dimensionless functions  $\hat{\Gamma}_{\text{fin}}^J(x_1)$  in Eq. (54) are defined by

$$\hat{\Gamma}_{\text{fin}}^0(x_1) = \int_{x_3^-}^{x_3^+} \frac{2(1-x_3)(8+x_3)C(x_1, x_3) + 3r(4-x_3)}{12(1-x_3)^2} \frac{dx_3}{x_3}, \quad (58a)$$

$$\hat{\Gamma}_{\text{fin}}^1(x_1) = -\frac{1}{3} \int_{x_3^-}^{x_3^+} C(x_1, x_3) \frac{dx_3}{x_3}, \quad (58b)$$

$$\hat{\Gamma}_{\text{fin}}^2(x_1) = \int_{x_3^-}^{x_3^+} \frac{(1-x_3)(5+x_3)C(x_1, x_3) + 3r(2-x_3)}{15(1-x_3)^2} \frac{dx_3}{x_3}, \quad (58c)$$

where  $C(x_1, x_3)$  is the function

$$C(x_1, x_3) = \frac{(1-x_1)^2 + (x_1+x_3-1)^2}{x_3^2}. \quad (59)$$

The results from carrying out the integrations over  $x_3$  in Eqs. (55) and (58) are tabulated in Appendix C.

To complete the matching calculation of the coefficient  $dA_J^{(c)}$ , we need to evaluate the NRQCD matrix element on the right side of the factorization formula in Eq. (17). The  $b\bar{b}$  states have a nonstandard normalization that corresponds to the procedure that we used in computing the full QCD rate  $d\Gamma[b\bar{b}_1(^3P_J) \rightarrow c + X]$  [Eqs. (23) and (42)]. Application of that procedure in NRQCD is equivalent to the use of  $b\bar{b}$  states that are normalized to  $3(2E_b)^2/\mathbf{q}^2$ , instead of the conventional  $(2E_b)^2$ , where  $\mathbf{q}$  is the momentum of the  $b$  quark in the quarkonium rest frame. The matrix element at leading order in the nonrelativistic approximation is then

$$\langle \mathcal{O}_1(^3P_J) \rangle_{b\bar{b}_1(^3P_J)} = 8N_c m_b^2. \quad (60)$$

Substituting Eqs. (40), (54), and (60) into the factorization formula (17), we obtain

$$\begin{aligned} dA_J^{(c)}(\Lambda) = & \frac{C_F \alpha_s^3}{N_c} c_3(\epsilon) \left( \frac{\Lambda^6}{m_b^4} \right)^\epsilon \left\{ \hat{\Gamma}_{\text{div}}^J(x_1) + \hat{\Gamma}_{\text{fin}}^J(x_1) \right. \\ & \left. + \left[ \frac{1}{\epsilon_{\text{IR}}} + \frac{2(r-1)}{3(2+r)} + \log \frac{m_b^2}{(1-r)\Lambda^2} \right] \frac{(2+r)\sqrt{1-r}}{9} \delta(1-x_1) \right\} dx_1 + O(\epsilon), \end{aligned} \quad (61)$$

where we use

$$(4\pi e^{-\gamma})^\epsilon \frac{c_2(\epsilon)}{c_3(\epsilon)} = 1 + O(\epsilon^2). \quad (62)$$

The explicit infrared divergence in Eq. (61) is canceled by the infrared divergence in  $\hat{\Gamma}_{\text{div}}^J(x_1)$ . Therefore the expression in Eq. (61) is finite at  $\epsilon = 0$ , and so we can neglect the  $\epsilon$  dependence in the prefactor. The only dependence on the scale  $\Lambda$  that remains appears in the bracket in Eq. (61).

It is now straightforward to determine the coefficients  $dA_J^{(c)}$ . Our final results for the

differential coefficients with respect to the energy fraction  $x_1$  of the charm quark are

$$\begin{aligned}
\frac{dA_0^{(c)}(\Lambda)}{dx_1} = & \frac{C_F \alpha_s^3}{N_c} \left\{ \left[ \left( \frac{2(2+r)}{9} \log \frac{4(1-\sqrt{r})m_b}{\sqrt{r}\Lambda} + \frac{1+r}{9} \right) \sqrt{1-r} \right. \right. \\
& \left. \left. - \frac{4+3r}{18} \log \frac{1+\sqrt{1-r}}{1-\sqrt{1-r}} \right] \delta(1-x_1) \right. \\
& + \frac{2}{9} \left( 28 - 35x_1 + (2+r) \left[ \frac{1}{1-x_1} \right]_{\sqrt{r}} \right) \sqrt{x_1^2 - r} \\
& + \left[ \frac{3}{2} + r - 3x_1(1-x_1) \right] \log \frac{x_1 + \sqrt{x_1^2 - r}}{x_1 - \sqrt{x_1^2 - r}} \\
& \left. - \frac{1}{6} \log \frac{2-x_1 + \sqrt{x_1^2 - r}}{2-x_1 - \sqrt{x_1^2 - r}} \right\}, \tag{63a}
\end{aligned}$$

$$\begin{aligned}
\frac{dA_1^{(c)}(\Lambda)}{dx_1} = & \frac{C_F \alpha_s^3}{N_c} \left\{ \left[ \left( \frac{2(2+r)}{9} \log \frac{4(1-\sqrt{r})m_b}{\sqrt{r}\Lambda} + \frac{1}{18} \right) \sqrt{1-r} \right. \right. \\
& \left. \left. - \frac{8+3r}{36} \log \frac{1+\sqrt{1-r}}{1-\sqrt{1-r}} \right] \delta(1-x_1) \right. \\
& + \frac{2}{9} \left( -\frac{1-5x_1}{2} + (2+r) \left[ \frac{1}{1-x_1} \right]_{\sqrt{r}} \right) \sqrt{x_1^2 - r} \\
& \left. - \frac{1}{3} \log \frac{2-x_1 + \sqrt{x_1^2 - r}}{2-x_1 - \sqrt{x_1^2 - r}} \right\}, \tag{63b}
\end{aligned}$$

$$\begin{aligned}
\frac{dA_2^{(c)}(\Lambda)}{dx_1} = & \frac{C_F \alpha_s^3}{N_c} \left\{ \left[ \left( \frac{2(2+r)}{9} \log \frac{4(1-\sqrt{r})m_b}{\sqrt{r}\Lambda} + \frac{7+4r}{90} \right) \sqrt{1-r} \right. \right. \\
& \left. \left. - \frac{40+21r}{180} \log \frac{1+\sqrt{1-r}}{1-\sqrt{1-r}} \right] \delta(1-x_1) \right. \\
& + \frac{2}{9} \left( \frac{73-89x_1}{10} + (2+r) \left[ \frac{1}{1-x_1} \right]_{\sqrt{r}} \right) \sqrt{x_1^2 - r} \\
& + \frac{2}{5} [1+r-2x_1(1-x_1)] \log \frac{x_1 + \sqrt{x_1^2 - r}}{x_1 - \sqrt{x_1^2 - r}} \\
& \left. - \frac{1}{15} \log \frac{2-x_1 + \sqrt{x_1^2 - r}}{2-x_1 - \sqrt{x_1^2 - r}} \right\}, \tag{63c}
\end{aligned}$$

where  $[1/(1-x_1)]_{\sqrt{r}}$  is the distribution defined in Eq. (57).

In Eq. (63), the terms involving the  $[1/(1-x_1)]_{\sqrt{r}}$  distribution diverge as  $1/(1-x_1)$  as  $x_1 \rightarrow 1$ . These singularities arise because, as  $x_1 \rightarrow 1$ , the energy of the real gluon in the final state goes to zero, giving rise to an infrared divergence in the rate. The second term in the definition of the  $[1/(1-x_1)]_{\sqrt{r}}$  distribution provides a negative contribution that cancels this divergence when one integrates over a region in  $x_1$  that contains the point  $x_1 = 1$ . Suppose that one integrates over the region  $x \leq x_1 \leq 1$ . Then, owing to the second term

in the definition of the  $[1/(1-x_1)]_{\sqrt{\tau}}$  distribution (57), the result is dominated in the limit  $x \rightarrow 1$  by a term that is proportional to  $-\log[1/(1-x)]$ . Such unphysical divergences are a symptom of the fact that the perturbation expansion in  $\alpha_s$  breaks down in the limit  $x_1 \rightarrow 1$  because of the appearance of large logarithms of  $1-x_1$ . A correct treatment of the region near  $x_1 = 1$  would involve the resummation of logarithms of  $1-x_1$  (Ref. [19–24]). As  $x \rightarrow 1$ , real gluon emission is suppressed. Hence, the resummation of logarithms of  $1-x$  generally leads to a Sudakov factor that suppresses the rate near  $x = 1$  (Ref. [19–24]). Consequently, as  $x \rightarrow 1$ , we expect the resummed distribution to turn over, rather than to diverge, and to approach zero smoothly at  $x = 1$ . We note that, in the rate integrated over all  $x_1$ , logarithms of  $1-x_1$  do not appear, and resummation is not necessary in order to obtain a reliable result.

In the limit  $x \rightarrow 1$ , the velocity expansion of NRQCD also breaks down because of kinematic constraints near the energy endpoint [25]. A correct treatment of this problem would involve the inclusion of shape functions [25] for the  $\chi_{bJ}$  mesons. In general, the inclusion of shape functions has the effect of smearing the energy distribution near the end point. We expect that these smearing effects will be important for  $1-x_1$  less than  $v \approx 0.3$ . In this region, the expression in Eq. (63) should not be taken as an accurate estimate of the distribution. (For a discussion of these effects in the decay of the  $\Upsilon$  meson into a photon plus light hadrons, see Ref. [26].) In the total rate integrated over  $x_1$ , the velocity expansion is well behaved and the effects from the shape function are of higher order in  $v^2$ .

The resummation of logarithms of  $1-x_1$  and the inclusion of shape functions are beyond the scope of this paper. In the absence of such analyses, one should treat our results with caution in the region near  $x_1 = 1$ .

### E. Charm-quark momentum distribution

The NRQCD factorization formula in Eq. (5) can be expressed in a form that is differential in the energy fraction  $x_1$  of the charm quark:

$$\frac{d\Gamma}{dx_1}[\chi_{bJ} \rightarrow c + X] = \frac{dA_J^{(c)}(\Lambda)}{dx_1} \frac{\langle \mathcal{O}_1 \rangle_{\chi_b}}{m_b^4} + \frac{dA_8^{(c)}}{dx_1} \frac{\langle \mathcal{O}_8 \rangle_{\chi_b}^{(\Lambda)}}{m_b^2}, \quad (64)$$

where the color-singlet coefficients  $dA_J^{(c)}(\Lambda)/dx_1$  are given in Eqs. (63) and the color-octet coefficient  $dA_8^{(c)}/dx_1$  is given in Eq. (41).

The momentum distribution for the charm quark can be obtained from Eq. (64) by a simple change of variables. It is convenient to express that momentum in terms of the fraction  $y_1$  of the maximum momentum for a charm quark that is kinematically allowed in the annihilation of a  $b\bar{b}$  pair at threshold:

$$y_1 = \sqrt{\frac{x_1^2 - r}{1 - r}}. \quad (65)$$

The range of  $y_1$  is  $0 < y_1 < 1$ . The inverse relation is

$$x_1 = \sqrt{(1 - r)y_1^2 + r}. \quad (66)$$

The distribution in the fractional momentum  $y_1$  can then be written as

$$\frac{d\Gamma}{dy_1} = \frac{(1 - r)y_1}{\sqrt{(1 - r)y_1^2 + r}} \frac{d\Gamma}{dx_1}. \quad (67)$$

The singular distribution  $[1/(1 - x_1)]_{\sqrt{r}}$  in the coefficients  $dA_J^{(c)}/dx_1$  in Eqs. (63) can be transformed into a singular distribution in the variable  $y_1$  as follows. From Eq. (57) we can derive the identity

$$\left[ \frac{1}{1 - x_1} \right]_{\sqrt{r}} dx_1 = \left\{ h(y_1) \left[ \frac{1}{1 - y_1} \right]_+ + \delta(1 - y_1) \int_0^1 dy' \frac{h(1) - h(y')}{1 - y'} \right\} dy_1, \quad (68)$$

where

$$h(y_1) = \left( \frac{1 - y_1}{1 - x_1} \right) \frac{dx_1}{dy_1}. \quad (69)$$

Note that  $h(1) = 1$ . Using Eq. (66) to compute  $h(y_1)$  and substituting the results into Eq. (68), we obtain

$$\left[ \frac{1}{1 - x_1} \right]_{\sqrt{r}} dx_1 = \left\{ \frac{y_1 [1 + \sqrt{(1 - r)y_1^2 + r}]}{(1 + y_1)\sqrt{(1 - r)y_1^2 + r}} \left[ \frac{1}{1 - y_1} \right]_+ + \log(1 + \sqrt{r})\delta(1 - y_1) \right\} dy_1, \quad (70)$$

where the plus distribution  $[1/(1 - y_1)]_+$  is defined by

$$\int_y^1 g(y_1) [f(y_1)]_+ dy_1 \equiv \int_y^1 [g(y_1) - g(1)] f(y_1) dy_1 - g(1) \int_0^y f(y_1) dy_1 \quad (71)$$

for any  $y$  in the interval  $0 \leq y < 1$  and any smooth function  $g(y_1)$ .

The charm-quark momentum distributions in the decays of  $\chi_{b0}$ ,  $\chi_{b1}$ , and  $\chi_{b2}$  are illustrated in Fig. 1. For the ratio  $r$ , which is defined in Eq. (37), we choose the value  $r = 4m_D^2/m_{\chi_{bJ}}^2$ ,

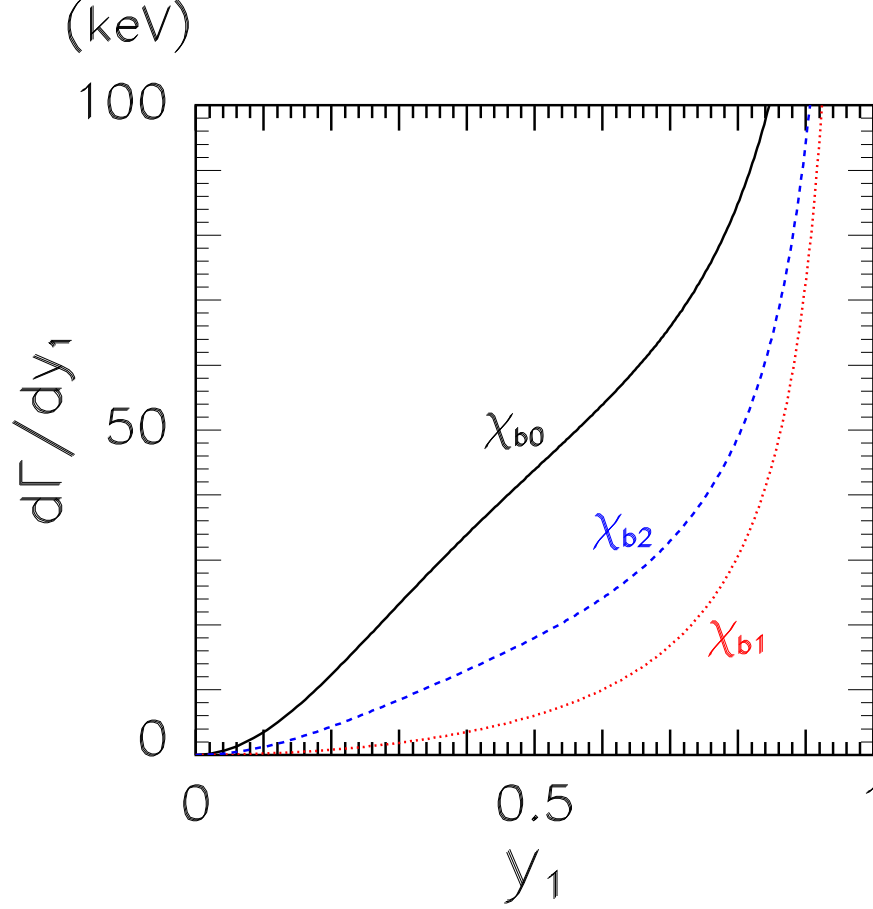


FIG. 1: Distribution of the scaled momentum  $y_1$  for the charm quark in decays of the  $\chi_{bJ}$  for  $J = 0$  (solid line), 1 (dotted line), and 2 (dashed line) for  $\alpha_s = 0.215$ ,  $\langle \mathcal{O}_1 \rangle_{\chi_b} = 2.03 \text{ GeV}^5$ , and  $m_b = 4.6 \text{ GeV}$ .

which is equivalent in the nonrelativistic approximation that we use in the calculation, but more correctly reflects the physical kinematics. Here,  $m_D$  is the average of the masses of the  $D^0$  and  $D^+$  and  $m_{\chi_{bJ}}$  is the mass of the  $\chi_{bJ}$  state.

If we use the most recent numerical values for the masses in Ref. [27], we find that this ratio is 0.1434, 0.1424, and 0.1419 for  $J = 0, 1$ , and 2, respectively, for the  $1P$  multiplet and 0.1331, 0.1325, and 0.1322 for  $J = 0, 1$ , and 2, respectively, for the  $2P$  multiplet. For  $y < 1$ , the color-octet terms in Eq. (64) do not contribute at leading order in  $\alpha_s$ . The normalizations of the momentum distributions for  $y < 1$  therefore depend only on the combination  $\alpha_s^3 \langle \mathcal{O}_1 \rangle_{\chi_b} / m_b^4$ . We choose  $\langle \mathcal{O}_1 \rangle_{\chi_b} \approx 2.03 \text{ GeV}^5$ , as is given in Eq. (8a). We take

the bottom-quark mass to be the one-loop pole mass:  $m_b = m_b^{(\text{pole})} \approx 4.6$  GeV. We take  $\alpha_s$  to be the running coupling constant at the scale  $m_b^{(\text{pole})}$ :  $\alpha_s \approx 0.215$ . The  $y_1$  distributions for  $\chi_{b0}$ ,  $\chi_{b1}$ , and  $\chi_{b2}$  in the  $1P$  multiplet are shown in Fig. 1. As is expected from our discussion in Sec. IIID, all three curves diverge as  $1/(1 - y_1)$  as  $y_1 \rightarrow 1$ . There are also singular distributions with support only at  $y_1 = 1$  that cannot be seen in the figure. As we have already mentioned, the singular distributions are such that the integrals of the  $y_1$  distributions over an interval in  $y_1$  that includes the endpoint  $y_1 = 1$  are finite.

## IV. TOTAL CHARM PRODUCTION RATE

### A. Short-distance coefficients

The inclusive charm production rate in decays of the  $\chi_{bJ}$  can be calculated by integrating the differential rate in Eq. (64). The integral of the color-octet coefficient in Eq. (41) is trivial:

$$A_8^{(c)} = \frac{(1 + r/2)\sqrt{1 - r}}{3} \pi \alpha_s^2. \quad (72)$$

The required integrals for the color-singlet coefficients in Eq. (63) are tabulated in Appendix D. These coefficients reduce to

$$A_0^{(c)}(\Lambda) = \frac{C_F \alpha_s^3}{N_c} \left\{ \left[ \frac{2(2 + r)}{9} \log \frac{8(1 - r)m_b}{r\Lambda} - \frac{58 + 23r}{27} \right] \sqrt{1 - r} + \frac{5}{9} \log \frac{1 + \sqrt{1 - r}}{1 - \sqrt{1 - r}} \right\}, \quad (73a)$$

$$A_1^{(c)}(\Lambda) = \frac{C_F \alpha_s^3}{N_c} \left\{ \left[ \frac{2(2 + r)}{9} \log \frac{8(1 - r)m_b}{r\Lambda} - \frac{16 + 11r}{27} \right] \sqrt{1 - r} - \frac{4}{9} \log \frac{1 + \sqrt{1 - r}}{1 - \sqrt{1 - r}} \right\}, \quad (73b)$$

$$A_2^{(c)}(\Lambda) = \frac{C_F \alpha_s^3}{N_c} \left\{ \left[ \frac{2(2 + r)}{9} \log \frac{8(1 - r)m_b}{r\Lambda} - \frac{116 + 91r}{135} \right] \sqrt{1 - r} - \frac{8}{45} \log \frac{1 + \sqrt{1 - r}}{1 - \sqrt{1 - r}} \right\}. \quad (73c)$$

### B. Comparison with previous results in the limit $m_c \rightarrow 0$

The limiting value of the color-octet coefficient  $A_8^{(c)}$  in Eq. (72) as  $r \rightarrow 0$  is  $\frac{1}{3} \pi \alpha_s^2$ , which agrees with the coefficient of  $n_f$  in the leading-order result for  $A_8$  in Eq. (3c). The limiting

behaviors of the color-singlet coefficients  $A_J^{(c)}$  as  $r \rightarrow 0$  are given by

$$A_0^{(c)}(\Lambda) \longrightarrow \frac{C_F \alpha_s^3}{N_c} \left( \log \frac{4}{r} + \frac{4}{9} \log \frac{2m_b}{\Lambda} - \frac{58}{27} \right), \quad (74a)$$

$$A_1^{(c)}(\Lambda) \longrightarrow \frac{C_F \alpha_s^3}{N_c} \left( \frac{4}{9} \log \frac{2m_b}{\Lambda} - \frac{16}{27} \right), \quad (74b)$$

$$A_2^{(c)}(\Lambda) \longrightarrow \frac{C_F \alpha_s^3}{N_c} \left( \frac{4}{15} \log \frac{4}{r} + \frac{4}{9} \log \frac{2m_b}{\Lambda} - \frac{116}{135} \right). \quad (74c)$$

The coefficients  $A_0^{(c)}$  and  $A_2^{(c)}$  in Eqs. (74) contain logarithms of  $r$ , and they therefore diverge in the limit  $m_c \rightarrow 0$ . In the inclusive decay rates of the  $\chi_{b0}$  and the  $\chi_{b2}$ , the logarithmic sensitivity of the short-distance coefficients to  $m_c$  is canceled by a correction to the decay rate for  $b\bar{b} \rightarrow gg$  from virtual  $c\bar{c}$  pairs. The corrections of order  $\alpha_s^3$  to the  $A_J$  from virtual charm quarks are given by

$$A_J^{(\text{virtual } c)} = -2i\Pi(0)A_J = \frac{2\alpha_s}{3\pi}A_J \log \frac{m_c}{\mu}, \quad (75)$$

where  $\Pi(k^2)$  is the  $\overline{\text{MS}}$ -subtracted quark-loop contribution to the gluon vacuum polarization at invariant four-momentum squared  $k^2$ , and the coefficients  $A_J$  that are nonzero at order  $\alpha_s^2$  are given in Eqs. (3). Then we have

$$A_0^{(\text{virtual } c)} = \frac{2C_F \alpha_s^3}{N_c} \log \frac{m_c}{\mu}, \quad (76a)$$

$$A_1^{(\text{virtual } c)} = 0, \quad (76b)$$

$$A_2^{(\text{virtual } c)} = \frac{8C_F \alpha_s^3}{15N_c} \log \frac{m_c}{\mu}. \quad (76c)$$

where  $\mu$  is the renormalization scale associated with regularizing the ultraviolet divergence of the quark-loop contributions to the gluon propagator. Upon adding these terms to the coefficients  $A_J^{(c)}$  in Eqs. (73), we see that the logarithmic dependence on  $m_c$  cancels and we can take the limit  $m_c \rightarrow 0$ . The sum of  $A_J^{(c)}$  and  $A_J^{(\text{virtual } c)}$  reduces in this limit to

$$\lim_{m_c \rightarrow 0} \left( A_0^{(c)} + A_0^{(\text{virtual } c)} \right) = \frac{C_F \alpha_s^3}{N_c} \left( 2 \log \frac{2m_b}{\mu} + \frac{4}{9} \log \frac{2m_b}{\Lambda} - \frac{58}{27} \right), \quad (77a)$$

$$\lim_{m_c \rightarrow 0} \left( A_1^{(c)} + A_1^{(\text{virtual } c)} \right) = \frac{C_F \alpha_s^3}{N_c} \left( \frac{4}{9} \log \frac{2m_b}{\Lambda} - \frac{16}{27} \right), \quad (77b)$$

$$\lim_{m_c \rightarrow 0} \left( A_2^{(c)} + A_2^{(\text{virtual } c)} \right) = \frac{C_F \alpha_s^3}{N_c} \left( \frac{8}{15} \log \frac{2m_b}{\mu} + \frac{4}{9} \log \frac{2m_b}{\Lambda} - \frac{116}{135} \right). \quad (77c)$$

These results agree with the coefficients of  $n_f$  in the next-to-leading-order calculation of  $A_J$  in Ref. [9], once one takes into account the different normalization convention for  $\langle \mathcal{O}_1 \rangle_{\chi_b}$  that is used in Ref. [9].

### C. Fraction of charm decays

The fraction  $R_J^{(c)}$  of the decays of  $\chi_{bJ}$  into light hadrons that include charm is given by the ratio of the NRQCD factorization formulas in Eqs. (5) and (2):

$$R_J^{(c)} = \frac{A_J^{(c)}(m_b) \langle \mathcal{O}_1 \rangle_{\chi_b} + A_8^{(c)} m_b^2 \langle \mathcal{O}_8 \rangle_{\chi_b}^{(m_b)}}{A_J(m_b) \langle \mathcal{O}_1 \rangle_{\chi_b} + A_8 m_b^2 \langle \mathcal{O}_8 \rangle_{\chi_b}^{(m_b)}}. \quad (78)$$

The short-distance coefficients in the numerator are given at leading order in  $\alpha_s$  in Eqs. (72) and (73). The short-distance coefficients in the denominator are given at leading order in  $\alpha_s$  in Eqs. (3) and (4). In Fig. 2, we show the fractions  $R_J^{(c)}$  as a functions of the dimensionless ratio  $\rho_8$  that is defined in Eq. (11). These fractions  $R_J^{(c)}$  are sufficiently sensitive to  $\rho_8$  that  $\rho_8$  could be determined phenomenologically from measurements of the inclusive branching fractions of the  $\chi_{bJ}$  into charm.

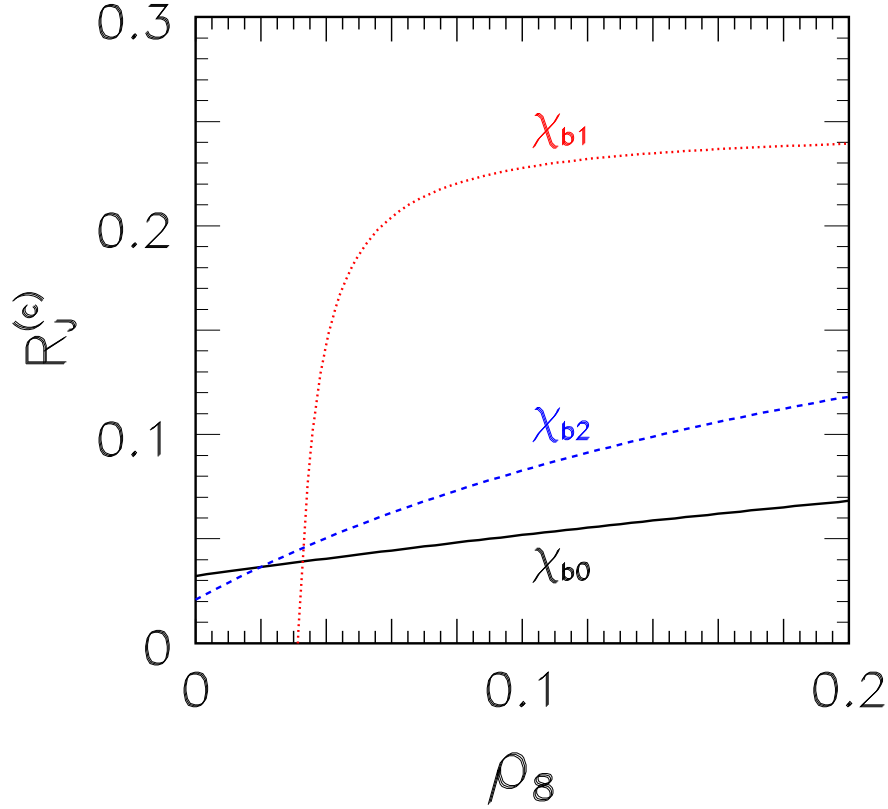


FIG. 2: Fractions  $R_J^{(c)}$  of the annihilation decays of the  $\chi_{bJ}$  that contain charm hadrons as functions of the ratio  $\rho_8 = m_b^2 \langle \mathcal{O}_8 \rangle_{\chi_b}^{(m_b)} / \langle \mathcal{O}_1 \rangle_{\chi_b}$  for  $J = 0$  (solid line), 1 (dotted line), and 2 (dashed line).

A simple physical constraint that can be imposed on the color-octet matrix element is

that both the numerator and denominator in Eq. (78) should be positive. If we use the leading-order approximations for the coefficients, then the strongest constraint comes from the positivity of the numerator for  $J = 1$ . This constraint requires that  $\rho_8 > 0.032$ .

## V. CHARM-MESON MOMENTUM DISTRIBUTION

In Sec. III, we calculated the momentum distribution of the charm quark in decays of the  $\chi_{b0}$ ,  $\chi_{b1}$ , and  $\chi_{b2}$ . Once it is created, a charm quark will hadronize with nearly 100% probability into a charm hadron. The charm hadron can be the  $D^0$ ,  $D^+$ ,  $D_s$ , or  $\Lambda_c$ , which are stable under strong and electromagnetic interactions, or it can be an excited charm hadron whose decay products include the  $D^0$ ,  $D^+$ ,  $D_s$ , or  $\Lambda_c$ . The effects of hadronization make the momentum spectrum of the charm hadron much softer than the momentum spectrum of the original charm quark.

The fragmentation of a charm quark into a charm hadron can be studied by using  $e^+e^-$  collisions. At leading order in  $\alpha_s$ , the production of a charm hadron in  $e^+e^-$  collisions with center-of-mass energy  $\sqrt{s}$  proceeds through the creation of a  $c$  and a  $\bar{c}$  with momenta  $\frac{1}{2}\sqrt{s - 4m_c^2}$ , followed by the fragmentation of the  $c$  into the charm hadron. Since the initial quark has a well-defined momentum, a measurement of the momentum distribution of the charm hadrons provides a measurement of the fragmentation process. The CLEO and Belle Collaborations have measured the momentum distributions of various charm hadrons in  $e^+e^-$  annihilation at center-of-mass energies near 10.6 GeV [28, 29]. This energy is fairly close to the masses of the  $\chi_b$  states, which are near 9.9 GeV for the  $1P$  multiplet and near 10.3 GeV for the  $2P$  multiplet. The results of Refs. [28, 29] show that the effects of hadronization are large. It is convenient to describe them in terms of the scaled momentum  $y$  that is obtained by dividing the momentum by its maximum possible value. At leading order in  $\alpha_s$ , the distribution for the charm quark is a Dirac delta function at  $y = 1$ . The peaks of the distributions in  $y$  for the charm hadrons measured in Ref. [29] range from 0.59 to 0.68.

A simple way to illustrate the effects of hadronization is to use a fragmentation approximation in which the charm-hadron momentum distribution is given by the convolution of the momentum distribution of the charm quark with a fragmentation function. The fragmentation function  $D_{c \rightarrow D}(z)$  gives the probability distribution for a charm quark with plus component of momentum  $E_1 + \mathbf{p}_1$  to hadronize into a charm hadron  $D$  with plus compo-

nent of momentum  $E_D + \mathbf{p}_D = z(E_1 + \mathbf{p}_1)$ . It is convenient to scale the plus component of momentum by its maximum possible value in the annihilation of  $b\bar{b}$  at threshold. The relation between the scaled plus component  $z_1$  and the scaled three-momentum  $y_1$  of the charm quark is

$$z_1 = \frac{\sqrt{(1-r)y_1^2 + r} + \sqrt{1-r}y_1}{1 + \sqrt{1-r}}. \quad (79)$$

The inverse relation is

$$y_1 = \frac{(1 + \sqrt{1-r})^2 z_1^2 - r}{2\sqrt{1-r}(1 + \sqrt{1-r})z_1}. \quad (80)$$

If we neglect the difference between the mass of the quark and the mass of the charm hadron, there are similar relations between the scaled components  $z_D$  and  $y_D$  of the four-momentum of the charm hadron. The fragmentation approximation for the momentum distribution of the charm hadron can then be written as

$$\begin{aligned} \frac{d\Gamma}{dy_D} &= \frac{dz_D}{dy_D} \int_{z_D}^1 \frac{dz_1}{z_1} D(z_D/z_1) \frac{dy_1}{dz_1} \frac{d\Gamma}{dy_1} \\ &= \frac{\sqrt{1-r}}{\sqrt{(1-r)y_D^2 + r}} \int_{y_D}^1 dy_1 \mathcal{D} \left( \frac{\sqrt{(1-r)y_D^2 + r} + \sqrt{1-r}y_D}{\sqrt{(1-r)y_1^2 + r} + \sqrt{1-r}y_1} \right) \frac{d\Gamma}{dy_1}, \end{aligned} \quad (81)$$

where  $\mathcal{D}(z) = zD(z)$ . The expression for  $d\Gamma/dy_D$  in Eq. (81), when integrated over  $y_D$ , does not preserve the normalization of the total cross section  $\int (d\Gamma/dy_1) dy_1$ , unless one takes the approximation of neglecting  $m_c$  in comparison to  $m_b$ , *i.e.* setting  $r = 0$ , in the relations (79) and (80) and in the limits of integration. In this approximation,  $z_1 = y_1$  and  $z_D = y_D$ . The change in the normalization of the total cross section is negative and is of order  $r$ . This change is at the level of the error in the fragmentation approximation itself, which is derived from QCD by neglecting corrections on the order of the square of the quark mass divided by the hard-scattering momentum [30].

The Belle Collaboration determined optimal values of the parameters for analytic parameterizations of the fragmentation functions for various charm hadrons by comparing their measured momentum distributions with the distributions predicted by Monte Carlo generators and fragmentation functions [29]. The best fits were obtained by using fragmentation functions that are functions of  $z$  and the transverse momentum  $p_\perp$ . Of the fragmentation functions that are functions of  $z$  only, the best fit was usually obtained by using the very simple Kartvelishvili fragmentation function:

$$D_{c \rightarrow D}(z) = N_D z^{\alpha_D} (1-z). \quad (82)$$

The fit for the  $D^+$  was better than that for the  $D^0$ , presumably because the momentum distribution for the  $D^+$  has smaller contributions from the feeddown from decays of the  $D^{*0}$  and the  $D^{*+}$ . For the  $D^+$ , the best fit for the exponent in Eq. (82) was  $\alpha_{D^+} = 4$ . The resulting fragmentation function has a peak at  $z = 0.8$ . The integral  $\int_0^1 dz D_{c \rightarrow D}(z)$  is the fragmentation probability for the charm hadron  $D$ . From Table X of Ref. [29], we can infer that the inclusive fragmentation probability for the  $D^+$ , including the feeddown from decays of the  $D^{*+}$ , is approximately 0.268. This fixes the normalization factor in Eq. (82) to be  $N_{D^+} = 8.04$ .

The fragmentation approximation to the  $D^+$  momentum distribution that is given by Eq. (81) is shown in Fig. 3, where the fragmentation function is given in Eq. (82). We have set  $r = 4m_D^2/m_{\chi_{bJ}}^2$ ,  $\alpha_s = \alpha_s(4.6 \text{ GeV}) = 0.215$ , and  $\langle \mathcal{O}_1 \rangle_{\chi_b} \approx 2.03 \text{ GeV}^5$ , as is given in Eq. (8a), and we have chosen  $\rho_8 = 0.1$ . Within the fragmentation approximation, the peaks in the momentum distributions of the  $D^+$  from decays of the  $\chi_{bJ}$  are at  $y_D = 0.53, 0.61$  and  $0.58$  for  $J = 0, 1$  and  $2$ , respectively. Also shown in Fig. 3 is the color-octet contribution to all three distributions, which peaks at  $y_D = 0.79$ . As we have mentioned above, the normalization of the total cross section decreases in the fragmentation approximation by an amount of order  $r$ . In the present case, the fragmentation approximation decreases the total cross sections by about 2.6%, 1.0%, and 1.9% for  $J = 0, 1$ , and  $2$ , respectively.

The momentum distributions in Fig. 3 have unphysical negative values near the endpoint at  $y_D = 1$ . The momentum distributions very near the endpoint are dominated by the  $[1/(1-x)]_{\sqrt{r}}$  terms in the coefficients  $dA_J^{(c)}(\Lambda)/dx_1$  in Eqs. (63). If we use Eq. (70) to transform the distribution in  $x_1$  into a distribution in  $y_1$ , then the negative terms come from the last term in the definition of  $[1/(1-y)]_+$  in Eq. (71). The limiting behavior as  $y_D \rightarrow 1$  from this term in the momentum distribution is

$$\frac{d\Gamma}{dy_D} \sim -D(z_D) \log \left( \frac{1}{1-y_D} \right) \frac{2(2+r)\sqrt{1-r}C_F\alpha_s^3\langle \mathcal{O}_1 \rangle_{\chi_b}}{9N_c m_b^4}. \quad (83)$$

If we use the Kartvelishvili fragmentation function [Eq. (82)], then all other terms in  $d\Gamma/dy_D$  vanish linearly in  $1-y_D$  as  $y_D \rightarrow 1$ . The fragmentation function  $D(z_D)$  in Eq. (83) also vanishes linearly in  $1-y_D$  as  $y_D \rightarrow 1$ , but the logarithm approaches  $-\infty$ , and so this negative term dominates sufficiently close to the end point.

As we mentioned with regard to the distributions in  $x_1$  in Sec. IIID, such unphysical contributions arise because, near  $y_D = 1$ , large logarithms of  $1-x_1$  cause the perturbation

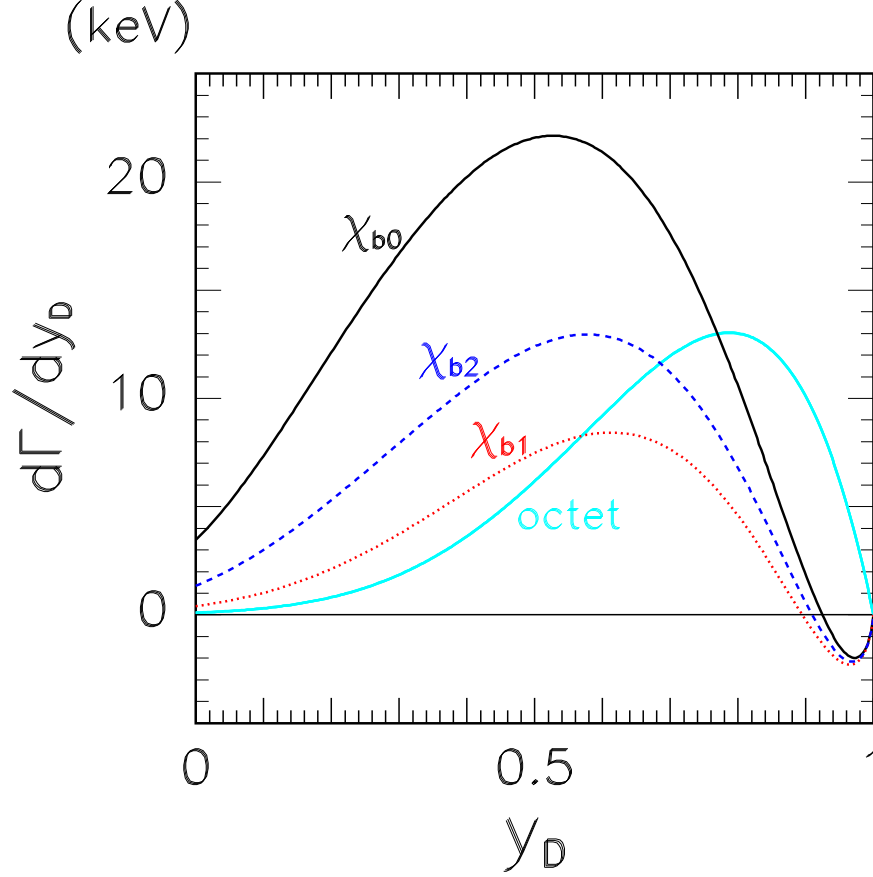


FIG. 3: Distribution of the scaled momentum  $y_D$  for the charm meson  $D^+$  in decays of the  $\chi_{bJ}$  for  $J = 0$  (solid line), 1 (dotted line), and 2 (dashed line) for  $\rho_8 = 0.1$ . Also shown is the color-octet contribution to the distributions (light solid line), which is the same, to within about 2 %, for  $J = 0, 1$ , and 2 and is already included in the other three curves. The unphysical negative behavior of the color-singlet contributions near the endpoint at  $y_D = 1$  might be eliminated by resumming logarithmic corrections to all orders, as is described in the text.

expansion in  $\alpha_s$  to break down. We expect that resummation of these logarithms to all orders in perturbation theory would cure the distribution in  $y_D$  of these unphysical effects.

## VI. SUMMARY

We have used the NRQCD factorization formalism to calculate the inclusive decay rate of the spin-triplet bottomonium states  $\chi_{bJ}$  into charm hadrons. In Eq. (5), the decay rates are

expressed in terms of two independent nonperturbative factors for each  $P$ -wave multiplet:  $\langle \mathcal{O}_1 \rangle_{\chi_b}$  and  $\langle \mathcal{O}_8 \rangle_{\chi_b}^{(\Lambda)}$ . The coefficients of these factors were calculated to leading order in  $\alpha_s$  using perturbative matching. Our results for the coefficients that are differential in the  $c$ -quark energy fraction are given in Eqs. (41) and (63). Our results for the coefficients integrated over the  $c$ -quark energy fraction are given in Eqs. (72) and (73). The ratios  $R_J^{(c)}$  of the decay rate of the  $\chi_{bJ}$  into light hadrons that include charm and the decay rate into all light hadrons are shown in Fig. 2 as a function of the ratio  $\rho_8$  of the NRQCD matrix elements. The ratios  $R_J^{(c)}$  are sufficiently sensitive to  $\rho_8$  that measurements of the branching fraction of the  $\chi_{bJ}$  into charm could be used to make a phenomenological determination of the  $\langle \mathcal{O}_8 \rangle_{\chi_b}^{(\Lambda)}$ . These matrix elements could then be used to predict the partial widths into light hadrons for all four states in the  $P$ -wave bottomonium multiplet.

We also calculated the momentum distribution of the charm quark from the decays of the  $\chi_{bJ}$ . We obtained a simple approximation to the momentum distribution for charm mesons in  $\chi_{bJ}$  decay by convolving the charm-quark momentum distribution with a fragmentation function for  $c \rightarrow D$  that was measured in  $e^+e^-$  collisions. The charm-meson momentum distributions for the  $\chi_{bJ}$  are shown in Fig. 3 as functions of the scaled momentum variable  $y_D$  for  $\rho_8 = 0.1$ . The CLEO-III experiment and the  $B$  factory experiments may be able to measure the momentum distributions of charm hadrons in  $\chi_{bJ}$  decay. One unsatisfactory aspect of the theoretical momentum distributions in Fig. 3 is the unphysical negative behavior of the distributions near the endpoint at  $y_D = 1$ . We expect that this difficulty could be overcome by resumming logarithmic corrections to all orders in  $\alpha_s$ . The region near the endpoint also receives large contributions that are formally of higher order in the NRQCD velocity expansion. Such contributions can be resummed to all orders in  $v$  by making use of a shape function. The completion of these resummation calculations would allow one to make quantitative comparisons between theoretical predictions and experimental measurements of the momentum distributions of the charm hadrons that are produced in  $\chi_{bJ}$  decays.

## Acknowledgments

We thank Roy Briere for suggesting this problem and for useful discussions. E. Braaten thanks KITP for its hospitality while this work was being completed. J. Lee thanks the High Energy Physics Theory Group at Argonne National Laboratory for its hospitality while this

work was carried out. Work by G. T. Bodwin in the High Energy Physics Division at Argonne National Laboratory is supported by the U. S. Department of Energy, Division of High Energy Physics, under Contract No. DE-AC02-06CH11357. The work of E. Braaten was supported in part by the U. S. Department of Energy, Division of High Energy Physics, under grant No. DE-FG02-91-ER40690. The work of D. Kang was supported by the Korea Research Foundation under grant KRF-2006-612-C00003. The work of J. Lee was supported by the Korea Research Foundation under MOEHRD Basic Research Promotion grant KRF-2006-311-C00020 and by the Basic Research Program of the Korea Science and Engineering Foundation (KOSEF) under grant No. R01-2005-000-10089-0.

## APPENDIX A: DIMENSIONALLY REGULARIZED THREE-BODY PHASE SPACE

In  $d = 4 - 2\epsilon$  space-time dimensions, the three-body phase space is defined by

$$d\Phi_3 = (2\pi)^d \delta^{(d)}(P - p_1 - p_2 - p_3) \frac{d^{d-1}p_1}{(2\pi)^{d-1}2E_1} \frac{d^{d-1}p_2}{(2\pi)^{d-1}2E_2} \frac{d^{d-1}p_3}{(2\pi)^{d-1}2E_3}, \quad (\text{A1})$$

where  $E_i$  and  $p_i$  are the energy and four-momentum of the particle  $i$  in the final state with mass  $m_i$ , and  $P = p_1 + p_2 + p_3$ . We evaluate  $d\Phi_3$  in the center-of-momentum frame,  $P = (\sqrt{P^2}, \mathbf{0})$ , where the resulting expressions are most compact. In any decay with a three-body final state, the squared matrix element, summed over spin states, is a Lorentz scalar, depending only on the four momenta  $P$ ,  $p_1$ ,  $p_2$ , and  $p_3$ . By using energy-momentum conservation, it can be seen that all possible scalar products of momenta can be expressed in terms of  $E_i$ 's. Therefore the spin-summed matrix element squared depends only on the energies  $E_i$ .

Integrating out  $\mathbf{p}_2$  and all angles except for the relative angle between  $\mathbf{p}_1$  and  $\mathbf{p}_3$ , we obtain

$$d\Phi_3 = \frac{(4\pi)^{2\epsilon} \Gamma\left(\frac{3}{2}\right)}{\Gamma(1-\epsilon)\Gamma\left(\frac{3}{2}-\epsilon\right)} \frac{(|\mathbf{p}_1||\mathbf{p}_3|)^{d-3}}{E_2} \sin^{d-4} \theta_{13} \delta(\sqrt{P^2} - E_1 - E_2 - E_3) \frac{dE_1 dE_3}{32\pi^3} d\cos \theta_{13}, \quad (\text{A2})$$

where  $\theta_{13}$  is the angle between  $\mathbf{p}_1$  and  $\mathbf{p}_3$  in the center-of-momentum frame. The angle  $\theta_{13}$  is fixed by the energy delta function:

$$E_2 = \sqrt{|\mathbf{p}_1|^2 + |\mathbf{p}_3|^2 + 2|\mathbf{p}_1||\mathbf{p}_3| \cos \theta_{13} + m_2^2}. \quad (\text{A3})$$

By solving Eq. (A3) in the center-of-momentum frame, we can express  $\sin^2 \theta_{13}$  in terms of the magnitudes of three-momenta for the final-state particles:

$$\sin^2 \theta_{13} = -\lambda(\mathbf{p}_1^2, \mathbf{p}_2^2, \mathbf{p}_3^2)/(4\mathbf{p}_1^2 \mathbf{p}_3^2), \quad (\text{A4})$$

where  $\lambda(x, y, z) = x^2 + y^2 + z^2 - 2(xy + yz + zx)$ . The physical region can be determined from the expression

$$-\lambda(\mathbf{p}_1^2, \mathbf{p}_2^2, \mathbf{p}_3^2) = (|\mathbf{p}_1| + |\mathbf{p}_2| + |\mathbf{p}_3|)(|\mathbf{p}_1| + |\mathbf{p}_2| - |\mathbf{p}_3|)(|\mathbf{p}_2| + |\mathbf{p}_3| - |\mathbf{p}_1|)(|\mathbf{p}_3| + |\mathbf{p}_1| - |\mathbf{p}_2|) > 0. \quad (\text{A5})$$

Substituting Eq. (A4) into Eq. (A2) and changing the integration variable from  $\cos \theta_{13}$  to  $E_2$ , using Eq. (A3), we obtain

$$d\Phi_3 = \frac{(4\pi)^{2\epsilon}}{\Gamma(2-2\epsilon)} \delta(\sqrt{P^2} - E_1 - E_2 - E_3) \frac{dE_1 dE_2 dE_3}{32\pi^3 [-\lambda(\mathbf{p}_1^2, \mathbf{p}_2^2, \mathbf{p}_3^2)]^\epsilon}. \quad (\text{A6})$$

In the calculations in this paper, we study the case  $p_1^2 = p_2^2 = m_c^2$ ,  $p_3^2 = 0$ , and  $\sqrt{P^2} = 2E_b$ . We express the energy variables in terms of dimensionless variables  $x_i = E_i/E_b$ . Then

$$\cos \theta_{13} = \frac{2E_b(E_b - E_1 - E_3) + E_1 E_3}{|\mathbf{p}_1| E_3} = \frac{(1 - x_1)/x_3 - a(x_1)}{b(x_1)}, \quad (\text{A7})$$

where  $a(x_1)$  and  $b(x_1)$  are defined by

$$a(x_1) = 1 - \frac{1}{2}x_1, \quad (\text{A8a})$$

$$b(x_1) = \frac{1}{2}\sqrt{x_1^2 - r}. \quad (\text{A8b})$$

The ranges of integrals are determined from Eq. (A5):

$$\sqrt{r} \leq x_1 \leq 1, \quad (\text{A9a})$$

$$x_3^- \leq x_3 \leq x_3^+, \quad (\text{A9b})$$

where  $x_3^\pm$  are defined by

$$x_3^\pm = \frac{1 - x_1}{a(x_1) \mp b(x_1)}. \quad (\text{A10})$$

## APPENDIX B: EVALUATION OF INTEGRALS $I_n(x_1)$

In this appendix, we evaluate the integrals  $I_n(x_1)$  that are defined in Eq. (56):

$$I_n(x_1) = \int_{x_3^-}^{x_3^+} \frac{(1 - x_1)^n dx_3}{x_3^{n+2+2\epsilon} (1 - \cos^2 \theta_{13})^\epsilon}. \quad (\text{B1})$$

where the bounds  $x_3^\pm$  of the integral are given in Eqs. (A8) and (A10). The cosine of the angle  $\theta_{13}$  is expressed as a function of  $x_1$  and  $x_3$  in Eq. (A7). By making the changes of variables

$$t = \frac{1 - x_1}{x_3} = a(x_1) + b(x_1) \cos \theta_{13} \quad (\text{B2})$$

and using the relation for  $\cos \theta_{13}$  in Eq. (A7), we can parametrize the  $I_n(x_1)$  as

$$\begin{aligned} I_n(x_1) &= \frac{1}{(1 - x_1)^{1+2\epsilon}} \int_{a(x_1)-b(x_1)}^{a(x_1)+b(x_1)} \frac{t^{n+2\epsilon} dt}{(1 - \cos^2 \theta_{13})^\epsilon} \\ &= \frac{b(x_1)}{(1 - x_1)^{1+2\epsilon}} \int_{-1}^1 \frac{[a(x_1) + b(x_1)x]^{n+2\epsilon} dx}{(1 - x^2)^\epsilon}. \end{aligned} \quad (\text{B3})$$

In the second line of Eq. (B3), we used Eq. (A7). It is evident that the  $t$  or  $x$  integrals in Eq. (B3) are finite. The divergent part is contained in the factor  $1/(1 - x_1)^{1+2\epsilon}$ , which is manifestly logarithmically divergent in the infrared limit  $x_1 \rightarrow 1$ . The integral of that factor over  $x_1$  is proportional to  $-1/(2\epsilon)$ . The evaluation of the integrals  $I_n(x_1)$ , keeping the full  $\epsilon$  dependence, is quite involved. However, in order to compute the pole in  $\epsilon$  and the finite term, we need only to expand the coefficient of  $1/(1 - x_1)^{1+2\epsilon}$  in Eq. (B3) to order  $\epsilon$ :

$$\begin{aligned} I_n(x_1) &= \frac{1}{(1 - x_1)^{1+2\epsilon}} \left\{ \int_{a(x_1)-b(x_1)}^{a(x_1)+b(x_1)} t^{n+2\epsilon} dt \right. \\ &\quad \left. - \epsilon b(x_1) \int_{-1}^1 [a(x_1) + b(x_1)x]^n \log(1 - x^2) dx \right\} + O(\epsilon) \\ &= \frac{1}{(1 - x_1)^{1+2\epsilon}} \left\{ \frac{[a(x_1) + b(x_1)]^{n+1+2\epsilon} - [a(x_1) - b(x_1)]^{n+1+2\epsilon}}{n + 1 + 2\epsilon} - 2\epsilon i_n(x_1) \right\} \\ &\quad + O(\epsilon), \end{aligned} \quad (\text{B4})$$

where the  $i_n(x_1)$  for  $n = 0, 1$ , and  $2$  are given by

$$i_0(x_1) = -2b(x_1)(1 - \log 2), \quad (\text{B5a})$$

$$i_1(x_1) = -2a(x_1)b(x_1)(1 - \log 2), \quad (\text{B5b})$$

$$i_2(x_1) = -2b(x_1) \left\{ \frac{1}{9}[b(x_1)]^2(4 - 3 \log 2) + [a(x_1)]^2(1 - \log 2) \right\}. \quad (\text{B5c})$$

It is convenient to rewrite the divergent integral as a linear combination of finite integrals and a singular integral involving a delta function. As we have noted, all the factors except for  $1/(1 - x_1)^{1+2\epsilon}$  are regular functions of  $x_1$ . We denote the factor that is the coefficient of

$1/(1-x_1)^{1+2\epsilon}$  by  $f(x_1)$ . Therefore, we wish to study the integral

$$I = \int_{\sqrt{r}}^1 \frac{f(x_1)dx_1}{(1-x_1)^{1+2\epsilon}}, \quad (\text{B6})$$

where  $f(x_1)$  is regular for any  $x_1 \in [\sqrt{r}, 1]$ . One can separate the divergent contributions to the integral from the finite piece as follows.

$$I = \int_{\sqrt{r}}^1 \frac{f(x_1) - f(1)}{(1-x_1)^{1+2\epsilon}} dx_1 + f(1) \int_{\sqrt{r}}^1 \frac{dx_1}{(1-x_1)^{1+2\epsilon}}. \quad (\text{B7})$$

The first term on the right side of Eq. (B7) is finite in the limit  $\epsilon \rightarrow 0$ . The second term on the right side of Eq. (B7) is singular in the limit  $\epsilon \rightarrow 0$ :

$$\int_{\sqrt{r}}^1 \frac{dx_1}{(1-x_1)^{1+2\epsilon}} = -\frac{1}{2\epsilon(1-\sqrt{r})^{2\epsilon}}. \quad (\text{B8})$$

Substituting Eq. (B8) into Eq. (B7), we obtain

$$I = \int_{\sqrt{r}}^1 dx_1 \left[ \frac{f(x_1) - f(1)}{(1-x_1)^{1+2\epsilon}} - \frac{f(1)\delta(1-x_1)}{2\epsilon(1-\sqrt{r})^{2\epsilon}} \right]. \quad (\text{B9})$$

Expanding the  $\epsilon$  dependence in the first term in Eq. (B9), we have

$$\frac{1}{(1-x_1)^{1+2\epsilon}} = -\frac{\delta(1-x_1)}{2\epsilon(1-\sqrt{r})^{2\epsilon}} + \left[ \frac{1}{1-x_1} \right]_{\sqrt{r}} - 2\epsilon \left[ \frac{\log(1-x_1)}{1-x_1} \right]_{\sqrt{r}} + O(\epsilon^2), \quad (\text{B10})$$

where the distribution  $[1/(1-x_1)]_{\sqrt{r}}$  is defined by Eq. (57). Retaining the first two terms in Eq. (B10), we obtain

$$\frac{I_0(x_1)}{(x_1^2 - r)^\epsilon} = \left[ \left( -\frac{1}{2\epsilon} + \log 2 \right) \sqrt{1-r} + L_0(r) \right] \delta(1-x_1) + \left[ \frac{1}{1-x_1} \right]_{\sqrt{r}} \sqrt{x_1^2 - r} + O(\epsilon), \quad (\text{B11a})$$

$$\begin{aligned} \frac{I_1(x_1)}{(x_1^2 - r)^\epsilon} = & \left[ \left( -\frac{1}{4\epsilon} - \frac{1}{4} + \frac{1}{2} \log 2 \right) \sqrt{1-r} + L_1(r) \right] \delta(1-x_1) \\ & + \left\{ \frac{1}{2} + \frac{1}{2} \left[ \frac{1}{1-x_1} \right]_{\sqrt{r}} \right\} \sqrt{x_1^2 - r} + O(\epsilon), \end{aligned} \quad (\text{B11b})$$

$$\begin{aligned} \frac{I_2(x_1)}{(x_1^2 - r)^\epsilon} = & \left\{ \left[ \left( -\frac{1}{24\epsilon} + \frac{1}{12} \log 2 \right) (4-r) - \frac{1}{4} + \frac{r}{12} \right] \sqrt{1-r} + L_2(r) \right\} \delta(1-x_1) \\ & + \left\{ \frac{2-x_1}{3} + \frac{4-r}{12} \left[ \frac{1}{1-x_1} \right]_{\sqrt{r}} \right\} \sqrt{x_1^2 - r} + O(\epsilon). \end{aligned} \quad (\text{B11c})$$

The functions  $L_n(r)$  are given by

$$L_n(r) = -\frac{1}{n+1} \left[ (a+b)^{n+1} \log(a+b) - (a-b)^{n+1} \log(a-b) \right] \\ + \frac{1}{2(n+1)} \left[ (a+b)^{n+1} - (a-b)^{n+1} \right] \log \left[ (1-\sqrt{r})^2(1-r) \right], \quad (\text{B12})$$

where  $a \pm b = a(1) \pm b(1) = \frac{1}{2}(1 \pm \sqrt{1-r})$ . These functions vanish in the massless limit  $r \rightarrow 0$ :  $L_n(0) = 0$ . The explicit expressions for  $L_0(r)$ ,  $L_1(r)$ , and  $L_2(r)$  are

$$L_0(r) = \frac{\sqrt{1-r}}{2} \log \frac{4(1-\sqrt{r})^2(1-r)}{r} - \frac{1}{2} \log \frac{1+\sqrt{1-r}}{1-\sqrt{1-r}}, \quad (\text{B13a})$$

$$L_1(r) = \frac{\sqrt{1-r}}{4} \log \frac{4(1-\sqrt{r})^2(1-r)}{r} - \frac{2-r}{8} \log \frac{1+\sqrt{1-r}}{1-\sqrt{1-r}}, \quad (\text{B13b})$$

$$L_2(r) = \frac{(4-r)\sqrt{1-r}}{24} \log \frac{4(1-\sqrt{r})^2(1-r)}{r} - \frac{4-3r}{24} \log \frac{1+\sqrt{1-r}}{1-\sqrt{1-r}}. \quad (\text{B13c})$$

### APPENDIX C: EVALUATION OF INTEGRALS OVER $x_3$

In this appendix, we report the results of carrying out the integrations over  $x_3$  in the components of the  $b\bar{b}$  differential widths in Eqs. (55) and (58).

The integrals  $I_n(x_1)$  that appear in the infrared-divergent functions  $\hat{\Gamma}_{\text{div}}^J(x_1)$  in Eqs. (55) are defined by integrals over  $x_3$  that are evaluated in Appendix B. Making use of these

results, we find that

$$\begin{aligned}\hat{\Gamma}_{\text{div}}^0(x_1) = & \left\{ \left( \frac{2(2+r)}{9} \left[ -\frac{1}{2\epsilon} + \log 2 \right] + \frac{5+r}{27} \right) \sqrt{1-r} \right. \\ & \left. + \frac{2+r}{3} L_0(r) - \frac{4}{3} [L_1(r) - L_2(r)] \right\} \delta(1-x_1) \\ & + \frac{2}{9} \left\{ 1 - 2x_1 + (2+r) \left[ \frac{1}{1-x_1} \right]_{\sqrt{r}} \right\} \sqrt{x_1^2 - r},\end{aligned}\tag{C1a}$$

$$\begin{aligned}\hat{\Gamma}_{\text{div}}^1(x_1) = & \left\{ \left( \frac{2(2+r)}{9} \left[ -\frac{1}{2\epsilon} + \log 2 \right] + \frac{7-4r}{54} \right) \sqrt{1-r} \right. \\ & \left. + \frac{2+r}{6} L_0(r) + \frac{2}{3} [L_1(r) - L_2(r)] \right\} \delta(1-x_1) \\ & + \frac{2}{9} \left\{ -\frac{1-2x_1}{2} + (2+r) \left[ \frac{1}{1-x_1} \right]_{\sqrt{r}} \right\} \sqrt{x_1^2 - r},\end{aligned}\tag{C1b}$$

$$\begin{aligned}\hat{\Gamma}_{\text{div}}^2(x_1) = & \left\{ \left( \frac{2(2+r)}{9} \left[ -\frac{1}{2\epsilon} + \log 2 \right] + \frac{41-8r}{270} \right) \sqrt{1-r} \right. \\ & \left. + \frac{7(2+r)}{30} L_0(r) - \frac{2}{15} [L_1(r) - L_2(r)] \right\} \delta(1-x_1) \\ & + \frac{2}{9} \left\{ \frac{1-2x_1}{10} + (2+r) \left[ \frac{1}{1-x_1} \right]_{\sqrt{r}} \right\} \sqrt{x_1^2 - r},\end{aligned}\tag{C1c}$$

where the distribution  $[1/(1-x_1)]_{\sqrt{r}}$  is defined in Eq. (71).

The infrared-finite functions  $\hat{\Gamma}_{\text{fin}}^J(x_1)$  in Eqs. (58) are defined by integrals over  $x_3$  that are straightforward to evaluate. The results of carrying out these integrations are

$$\begin{aligned}\hat{\Gamma}_{\text{fin}}^0(x_1) = & \frac{2\sqrt{x_1^2 - r}}{3} (9 - 11x_1) + \left[ \frac{3}{2} + r - 3x_1(1-x_1) \right] \log \frac{x_1 + \sqrt{x_1^2 - r}}{x_1 - \sqrt{x_1^2 - r}} \\ & - \frac{1}{6} \log \frac{2 - x_1 + \sqrt{x_1^2 - r}}{2 - x_1 - \sqrt{x_1^2 - r}},\end{aligned}\tag{C2a}$$

$$\hat{\Gamma}_{\text{fin}}^1(x_1) = \frac{x_1 \sqrt{x_1^2 - r}}{3} - \frac{1}{3} \log \frac{2 - x_1 + \sqrt{x_1^2 - r}}{2 - x_1 - \sqrt{x_1^2 - r}},\tag{C2b}$$

$$\begin{aligned}\hat{\Gamma}_{\text{fin}}^2(x_1) = & \frac{\sqrt{x_1^2 - r}}{15} (24 - 29x_1) + \frac{2}{5} [1 + r - 2x_1(1-x_1)] \log \frac{x_1 + \sqrt{x_1^2 - r}}{x_1 - \sqrt{x_1^2 - r}} \\ & - \frac{1}{15} \log \frac{2 - x_1 + \sqrt{x_1^2 - r}}{2 - x_1 - \sqrt{x_1^2 - r}}.\end{aligned}\tag{C2c}$$

## APPENDIX D: EVALUATION OF INTEGRALS OVER $x_1$

In this appendix, we tabulate the integrals that are required to obtain the inclusive short-distance coefficients  $A_J^{(c)}$  in Eq. (73) from the short-distance coefficients  $dA_J^{(c)}$  in Eq. (63) that are differential in  $x_1$ .

Some of the basic integrals over  $x_1$  are

$$\int_{\sqrt{r}}^1 dx_1 x_1 \sqrt{x_1^2 - r} = \frac{1}{3}(1-r)^{3/2}, \quad (\text{D1a})$$

$$\int_{\sqrt{r}}^1 dx_1 \sqrt{x_1^2 - r} = \frac{\sqrt{1-r}}{2} - \frac{r}{4} \log \frac{1+\sqrt{1-r}}{1-\sqrt{1-r}}, \quad (\text{D1b})$$

$$\begin{aligned} \int_{\sqrt{r}}^1 dx_1 \sqrt{x_1^2 - r} \left[ \frac{1}{1-x_1} \right]_{\sqrt{r}} &= -\sqrt{1-r} \left[ 1 + \frac{1}{2} \log \frac{r}{4} - \log(1+\sqrt{r}) \right] \\ &\quad - \frac{1}{2} \log \frac{1+\sqrt{1-r}}{1-\sqrt{1-r}}. \end{aligned} \quad (\text{D1c})$$

The integrals over  $x_1$  of the infrared-divergent functions  $\hat{\Gamma}_{\text{div}}^J(x_1)$  given in Eq. (C1) are

$$\begin{aligned} \int_{\sqrt{r}}^1 dx_1 \hat{\Gamma}_{\text{div}}^0(x_1) &= \frac{2(2+r)}{9} \left[ -\frac{1}{2\epsilon} - \log \frac{r}{8} + 3 \log \sqrt{1-r} \right] \sqrt{1-r} \\ &\quad - \frac{8+r}{27} \sqrt{1-r} - \frac{4+3r}{9} \log \frac{1+\sqrt{1-r}}{1-\sqrt{1-r}}, \end{aligned} \quad (\text{D2a})$$

$$\begin{aligned} \int_{\sqrt{r}}^1 dx_1 \hat{\Gamma}_{\text{div}}^1(x_1) &= \frac{2(2+r)}{9} \left[ -\frac{1}{2\epsilon} - \log \frac{r}{8} + 3 \log \sqrt{1-r} \right] \sqrt{1-r} \\ &\quad - \frac{2(4+5r)}{27} \sqrt{1-r} - \frac{8+3r}{18} \log \frac{1+\sqrt{1-r}}{1-\sqrt{1-r}}, \end{aligned} \quad (\text{D2b})$$

$$\begin{aligned} \int_{\sqrt{r}}^1 dx_1 \hat{\Gamma}_{\text{div}}^2(x_1) &= \frac{2(2+r)}{9} \left[ -\frac{1}{2\epsilon} - \log \frac{r}{8} + 3 \log \sqrt{1-r} \right] \sqrt{1-r} \\ &\quad - \frac{8(5+4r)}{135} \sqrt{1-r} - \frac{40+21r}{90} \log \frac{1+\sqrt{1-r}}{1-\sqrt{1-r}}. \end{aligned} \quad (\text{D2c})$$

The integrals over  $x_1$  of the infrared-finite functions  $\hat{\Gamma}_{\text{fin}}^J(x_1)$  given in Eq. (C2) are

$$\int_{\sqrt{r}}^1 dx_1 \hat{\Gamma}_{\text{fin}}^0(x_1) = -\frac{8(2+r)}{9} \sqrt{1-r} + \frac{3+r}{3} \log \frac{1+\sqrt{1-r}}{1-\sqrt{1-r}}, \quad (\text{D3a})$$

$$\int_{\sqrt{r}}^1 dx_1 \hat{\Gamma}_{\text{fin}}^1(x_1) = -\frac{2+r}{9} \sqrt{1-r} + \frac{r}{6} \log \frac{1+\sqrt{1-r}}{1-\sqrt{1-r}}, \quad (\text{D3b})$$

$$\int_{\sqrt{r}}^1 dx_1 \hat{\Gamma}_{\text{fin}}^2(x_1) = -\frac{22+23r}{45} \sqrt{1-r} + \frac{8+7r}{30} \log \frac{1+\sqrt{1-r}}{1-\sqrt{1-r}}. \quad (\text{D3c})$$

- 
- [1] R. Barbieri, R. Gatto, and R. Kogerler, Phys. Lett. **60B**, 183 (1976).
  - [2] R. Barbieri, R. Gatto, and E. Remiddi, Phys. Lett. **61B**, 465 (1976).
  - [3] R. Barbieri, M. Caffo, R. Gatto, and E. Remiddi, Nucl. Phys. **B192**, 61 (1981).
  - [4] G. T. Bodwin, E. Braaten, and G. P. Lepage, Phys. Rev. D **46**, R1914 (1992) [arXiv:hep-lat/9205006].
  - [5] G. T. Bodwin, E. Braaten, and G. P. Lepage, Phys. Rev. D **51**, 1125 (1995) [Erratum-ibid. D **55**, 5853 (1997)] [arXiv:hep-ph/9407339].
  - [6] H. Fritzsch and K. H. Streng, Phys. Lett. **77B**, 299 (1978).
  - [7] R. Barbieri, M. Caffo, and E. Remiddi, Phys. Lett. **83B**, 345 (1979).
  - [8] H. W. Huang, H. M. Hu, and X. F. Zhang, Phys. Rev. D **56**, 5816 (1997).
  - [9] A. Petrelli, M. Cacciari, M. Greco, F. Maltoni, and M. L. Mangano, Nucl. Phys. **B514**, 245 (1998) [arXiv:hep-ph/9707223].
  - [10] H. W. Huang and K. T. Chao, Phys. Rev. D **54**, 6850 (1996) [Erratum-ibid. D **56**, 1821 (1997)] [arXiv:hep-ph/9606220].
  - [11] G. T. Bodwin, D. K. Sinclair, and S. Kim, Phys. Rev. Lett. **77**, 2376 (1996) [arXiv:hep-lat/9605023].
  - [12] G. T. Bodwin, D. K. Sinclair, and S. Kim, Phys. Rev. D **65**, 054504 (2002) [arXiv:hep-lat/0107011].
  - [13] E. J. Eichten and C. Quigg, Phys. Rev. D **52**, 1726 (1995) [arXiv:hep-ph/9503356].
  - [14] G. T. Bodwin, D. Kang, and J. Lee, Phys. Rev. D **74**, 014014 (2006) [arXiv:hep-ph/0603186].
  - [15] N. Brambilla, D. Eiras, A. Pineda, J. Soto, and A. Vairo, Phys. Rev. Lett. **88**, 012003 (2002) [arXiv:hep-ph/0109130].
  - [16] J. H. Kuhn, J. Kaplan and E. G. O. Safiani, Nucl. Phys. **B157**, 125 (1979).
  - [17] B. Guberina, J. H. Kuhn, R. D. Peccei and R. Ruckl, Nucl. Phys. **B174**, 317 (1980).
  - [18] G. T. Bodwin and A. Petrelli, Phys. Rev. D **66**, 094011 (2002) [arXiv:hep-ph/0205210].
  - [19] C. W. Bauer, S. Fleming and M. E. Luke, Phys. Rev. D **63**, 014006 (2001) [arXiv:hep-ph/0005275].
  - [20] C. W. Bauer, C. W. Chiang, S. Fleming, A. K. Leibovich, and I. Low, Phys. Rev. D **64**, 114014 (2001) [arXiv:hep-ph/0106316].

- [21] S. Fleming and A. K. Leibovich, Phys. Rev. Lett. **90**, 032001 (2003) [arXiv:hep-ph/0211303].
- [22] S. Fleming and A. K. Leibovich, Phys. Rev. D **67**, 074035 (2003) [arXiv:hep-ph/0212094].
- [23] S. Fleming and A. K. Leibovich, Phys. Rev. D **70**, 094016 (2004) [arXiv:hep-ph/0407259].
- [24] S. Fleming, C. Lee, and A. K. Leibovich, Phys. Rev. D **71**, 074002 (2005) [arXiv:hep-ph/0411180].
- [25] M. Beneke, I. Z. Rothstein, and M. B. Wise, Phys. Lett. B **408**, 373 (1997) [arXiv:hep-ph/9705286].
- [26] X. Garcia i Tormo and J. Soto, Phys. Rev. D **72**, 054014 (2005) [arXiv:hep-ph/0507107].
- [27] W. M. Yao *et al.* (Particle Data Group), J. Phys. G **33**, 1 (2006).
- [28] M. Artuso *et al.* (CLEO Collaboration), Phys. Rev. D **70**, 112001 (2004) [arXiv:hep-ex/0402040].
- [29] R. Seuster *et al.* (Belle Collaboration), Phys. Rev. D **73**, 032002 (2006) [arXiv:hep-ex/0506068].
- [30] J. C. Collins, D. E. Soper, and G. Sterman, in *Perturbative QCD*, edited by A. H. Mueller, Advanced Series on Directions in High Energy Physics (World Scientific, Singapore, 1989), Vol. 5 [arXiv:hep-ph/0409313].